Assessing offsets between the $\delta^{13}C$ of sedimentary components and the global exogenic carbon pool across early Paleogene carbon cycle perturbations

Appy Sluijs[1] and Gerald R. Dickens[1,2]

Received 28 September 2011; revised 27 April 2012; accepted 20 August 2012; published 18 October 2012.

[1] Negative stable carbon isotope excursions (CIEs) across the Paleocene–Eocene thermal maximum (PETM; ~56 Ma) range between 2‰ and 7‰, even after discounting sections with truncated records. Individual carbon isotope records differ in shape and magnitude from variations in the global exogenic carbon cycle through changes in (1) the relative abundance of mixed components with different $\delta^{13}C$ within a measured substrate, (2) isotope fractionation through physiological change, and (3) the isotope composition of the carbon source. All three factors likely influence many early Paleogene $\delta^{13}C$ records, especially across the PETM and other hyperthermal events. We apply these concepts to late Paleocene–early Eocene (~58–52 Ma) records from Lomonosov Ridge, Arctic Ocean. Linear regression analyses show correlations between the $\delta^{13}C$ of total organic carbon (TOC) and two proxies for the relative contribution of terrestrial organic components to sediment TOC: the branched and isoprenoid tetraether index and palynomorphs. We use these correlations to subtract the terrestrial component from $\delta^{13}C_{TOC}$ and calculate marine organic matter $\delta^{13}C$. The results show that the magnitude of the CIE in $\delta^{13}C_{TOC}$ across the PETM is exaggerated relative to the magnitude of the CIE in $\delta^{13}C_{MOM}$ by ~3‰ due to increased contributions of terrestrial organic carbon during the event. Collectively, all carbon isotope records across the PETM and other major climate–carbon cycle perturbations in Earth's history are potentially biased through one or more of the above factors. Indeed, it is highly unlikely that any $\delta^{13}C$ record shows the true shape and magnitude of the CIE for the global exogenic carbon cycle. For the PETM, we conclude that CIE in the exogenic carbon cycle is likely <4‰, but it will take additional analyses and modeling to obtain an accurate value for this CIE.

Citation: Sluijs, A., and G. R. Dickens (2012), Assessing offsets between the $\delta^{13}C$ of sedimentary components and the global exogenic carbon pool across early Paleogene carbon cycle perturbations, *Global Biogeochem. Cycles*, *26*, GB4005, doi:10.1029/2011GB004224.

1. Introduction

[2] Earth's surface, especially at high latitudes and in the deep sea, experienced warming from the late Paleocene through the early Eocene (~59–51 Ma) [*Zachos et al.*, 2008]. Evidence for this warming comes from microfossil biogeography [e.g., *Adams et al.*, 1990; *Thomas and Shackleton*, 1996; *Bujak and Brinkhuis*, 1998] and sediment chemistry, such as foraminiferal $\delta^{18}O$ or TEX_{86} records [e.g., *Zachos et al.*, 2001; *Pearson et al.*, 2007; *Bijl et al.*, 2009]. The temperature increase broadly corresponded to a decrease in the $\delta^{13}C$ of carbon-bearing phases (Figure 1) [*Shackleton*, 1986; *Stein et al.*, 2006; *Hilting et al.*, 2008; *Zachos et al.*, 2008; *Zachos et al.*, 2010], and a deepening of carbonate saturation horizons in the ocean [*Hancock et al.*, 2007; *Leon-Rodriguez and Dickens*, 2010]. Both suggest a large, multimillion-year rise in ocean and atmosphere carbon contents.

[3] Superimposed on these long-term trends were several "hyperthermals," relatively brief (<200 kyr) events characterized by significant additional warming [e.g., *Bowen et al.*, 2006; *Sluijs et al.*, 2007a]. The Paleocene–Eocene thermal maximum (PETM; ~56 Ma) is the most prominent and best studied example, but at least six other episodes (e.g., Eocene thermal maximum 2, ETM2; ~54 Ma) now clearly manifest in multiple sediment sequences from widespread locations [e.g., *Cramer et al.*, 2003; *Lourens et al.*, 2005; *Nicolo et al.*, 2007]. While their number and absolute ages remain uncertain, the hyperthermals each exhibit a negative stable carbon isotope excursion (CIE) in various sedimentary components (Figure 1), and dissolution of carbonate in deep ocean basins

[1]Laboratory of Palaeobotany and Palynology, Department of Earth Sciences, Faculty of Geosciences, Utrecht University, Utrecht, Netherlands.
[2]Department of Earth Sciences, Rice University, Houston, Texas, USA.

Corresponding author: A. Sluijs, Laboratory of Palaeobotany and Palynology, Department of Earth Sciences, Faculty of Geosciences, Utrecht University, Budapestlaan 4, NL-3584 CD Utrecht, Netherlands. (a.sluijs@uu.nl)

0886-6236/12/2011GB004224

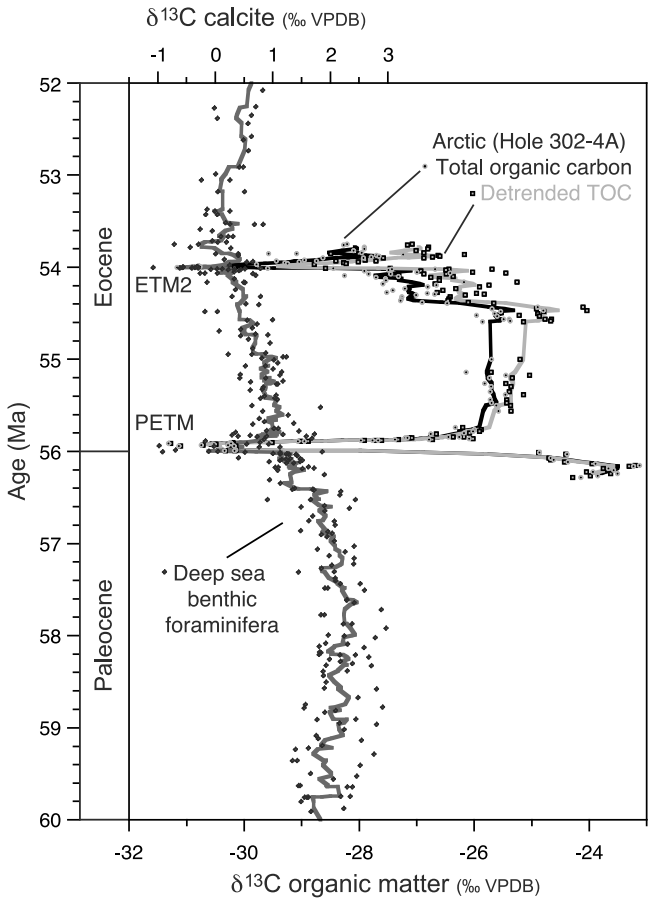

Figure 1. Comparison of deep-sea benthic foraminifer δ^{13}C and Hole 302-4A $\delta^{13}C_{TOC}$ records between 51 and 59 Ma. Left graph represents benthic foraminifer δ^{13}C values compiled by *Zachos et al.* [2008], complemented with the *Cibicidoides* data for ETM2 from *Lourens et al.* [2005]. Lines are five-point moving averages. VPDB = Vienna Peedee belemnite. The Hole 302-4A $\delta^{13}C_{TOC}$ record is detrended for global exogenic trends (gray line; see section 4.2) using the long-term trend in benthic foraminifer δ^{13}C.

[e.g., *Zachos et al.*, 2005; *Stap et al.*, 2009]. These observations, along with the relative timing and magnitude of CIEs, are best explained by a series of geologically rapid and massive injections of ^{13}C-depleted carbon from some carbon reservoir, or "carbon capacitor" [*Dickens*, 2000, 2003] into the exogenic carbon pool [*Dickens et al.*, 1997; *Panchuk et al.*, 2008; *Zeebe et al.*, 2009]. The latter, where carbon would cycle on geologically short ($\sim 10^3$ years) time scales, would comprise the ocean, atmosphere, and terrestrial biosphere, including soil and humus [*Kump and Arthur*, 1999]. The capacitor would slowly store massive amounts of ^{13}C-depleted carbon over relatively long (10^5–10^6 years) time scales but could release such carbon relatively quickly ($<10^5$ years) upon environmental change [*Dickens*, 2003]. Such systems might include seafloor gas hydrate systems [*Dickens*, 2003], peat [*Kurtz et al.*, 2003], or permafrost [*DeConto et al.*, 2012].

[4] The late Paleocene to early Eocene presents an especially intriguing interval for studying past climate change and carbon cycling [*Zachos et al.*, 2008]. A series of slow and fast net carbon inputs to the exogenic carbon cycle occurred and these additions coincided with a range of environmental responses [*Adams et al.*, 1990; *Bujak and Brinkhuis*, 1998; *Bowen et al.*, 2006; *Sluijs et al.*, 2007a; *McInerney and Wing*, 2011]. Furthermore, the superposition of the short-term injection events upon long-term changes implies different boundary states in which to examine the climate system and carbon cycling. Within this context, determining the magnitude and timing of changes in the δ^{13}C of the exogenic carbon cycle becomes an important goal, because these constrain the size and source of the carbon injections from the inferred capacitor [e.g., *Dickens et al.*, 1997; *Kump and Arthur*, 1999; *Dickens*, 2001; *Panchuk et al.*, 2008; *Zeebe et al.*, 2009].

[5] Perhaps 100 δ^{13}C records, using a range of carbon substrates, have been generated across the PETM to date [*McInerney and Wing*, 2011]. Moreover, δ^{13}C records are rapidly emerging across the other hyperthermals [*Cramer et al.*, 2003; *Lourens et al.*, 2005; *Nicolo et al.*, 2007; *Sluijs et al.*, 2009; *Stap et al.*, 2009, 2010; *Clementz et al.*, 2011; *Abels et al.*, 2012]. The shapes and magnitudes of CIEs in these records vary significantly [*Bowen et al.*, 2004; *Stoll*, 2005; *Schouten et al.*, 2007], which raises a provocative question: how do δ^{13}C variations in any of these records relate to changes in the δ^{13}C of the exogenic carbon cycle as a whole? We present and discuss mechanisms that may bias individual records and put these into a conceptual framework. We then discuss how δ^{13}C records of total organic carbon ($\delta^{13}C_{TOC}$) records may be corrected for changing organic matter composition across hyperthermal records, using published records from Integrated Ocean Drilling Program Hole 302-4A on Lomonosov Ridge, Arctic Ocean (Figure 2), as an example.

2. The Carbon Cycle Recording Problem

[6] For about two decades, it has been generally accepted that a prominent negative CIE marks the stratigraphic position of the PETM in sedimentary sections worldwide [*Kennett and Stott*, 1991; *Koch et al.*, 1992]. The CIE can be described, in a basic sense, as a major drop in δ^{13}C over a fairly short interval of stratigraphic depth (time) followed by substantial rise in δ^{13}C over a somewhat longer interval of stratigraphic depth (time). Although the exact timing remains controversial, all interpretations derived from multiple approaches indicate the entire CIE (onset and partial recovery) occurred within 220 kyr [*Röhl et al.*, 2007; *Abdul Aziz et al.*, 2008; *Murphy et al.*, 2010].

[7] The CIE is widely regarded to represent a massive input of ^{13}C-depleted CO_2 to the exogenic carbon cycle, followed by uptake of excess carbon into one or more reservoirs. This idea initially arose from considerations of the size, shape and approximate timing of the CIE [*Dickens et al.*, 1995; *Thomas and Shackleton*, 1996; *Dickens et al.*, 1997], as well as its occurrence in sediment records from different carbon reservoirs, notably the shallow and deep ocean [*Kennett and Stott*, 1991; *Pak and Miller*, 1992] and soils [*Koch et al.*, 1992]. The source of the CO_2, including whether it was oxidized CH_4, remains contentious [*Dickens et al.*, 1995; *Kurtz et al.*, 2003; *Svensen et al.*, 2004]. Nonetheless, confirmation for the general carbon injection hypothesis has come from the numerous δ^{13}C records generated since [*McInerney and Wing*, 2011], as well from carbonate accumulation records in deep-

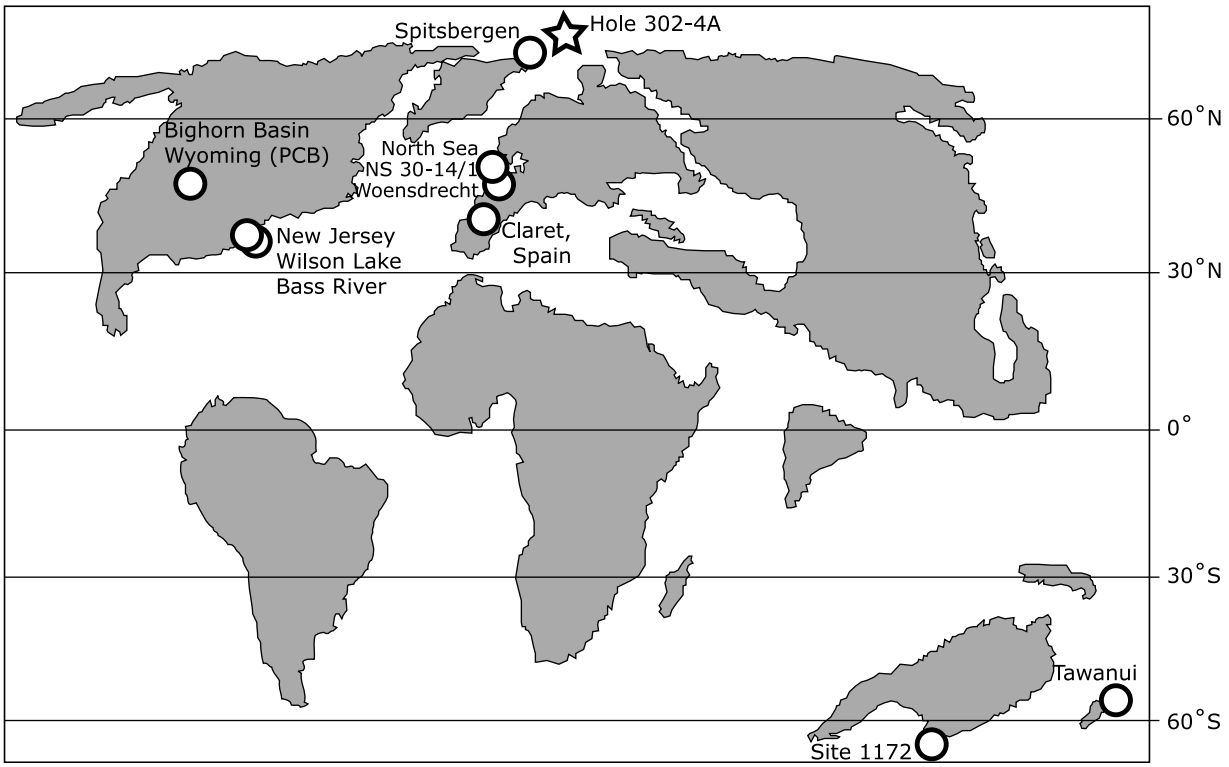

Figure 2. Locations of the discussed sites within a paleogeographic reconstruction of early Eocene times. Modified from *Scotese and Golanka* [1992].

sea sediment sequences, which show carbonate dissolution at the onset of the PETM, followed by very high carbonate preservation toward the end of the event [*Kelly et al.*, 2005; *Zachos et al.*, 2005]. These are expected geological expressions for a massive input of CO_2 to the ocean, atmosphere or both [*Dickens et al.*, 1997].

[8] Theoretically, the magnitude and timing for such a global negative CIE should relate to a few basic parameters [e.g., *Kump and Arthur*, 1999; *Dickens*, 2001]: the mass and δ^{13}C of the exogenic carbon cycle prior to the carbon injection, the size and δ^{13}C of carbon fluxes into and out of the exogenic carbon reservoirs before the perturbation, and the changes in carbon fluxes during the event. Several issues arise, however, when one attempts to transfer this conceptual framework to the geological record. For example, δ^{13}C records of various carbon-bearing phases in PETM sediment sections show a very large variation in the magnitude of the CIE, between 2‰ and 7‰, depending on location and analyzed substrate [*McInerney and Wing*, 2011]. In some sections, such variations result from brief hiatuses or core recovery problems at the onset of the event, which can lead to an absence of the recording substrate. Clearly, seafloor dissolution has truncated some marine carbonate δ^{13}C records [*McCarren et al.*, 2009]. However, variations in the size of the CIE remain even after discounting sections with record gaps. For example, a ~2‰ CIE manifests in bulk carbonate δ^{13}C records across an expanded and continuous PETM section at Mead Stream, New Zealand [*Hollis et al.*, 2005a]. A similar change is found in a bulk carbonate δ^{13}C record at Maud Rise, South Atlantic, where the record also appears continuous [*Bains et al.*, 1999]. However, at this location, benthic foraminifera, thermocline dwelling foraminifera, and mixed layer dwelling foraminifera display CIEs of 2.5‰, 2‰, and 4.5‰, respectively [*Kennett and Stott*, 1991; *Thomas et al.*, 2002; *Kelly et al.*, 2005].

[9] The magnitude and timing of a negative δ^{13}C excursion caused by a massive carbon input should show small variations between different pools of the exogenic carbon cycle [*Dickens*, 2000]. This is because δ^{13}C changes along flow paths away from potential sites of carbon injection, a phenomenon that can be demonstrated using carbon cycle models that track the δ^{13}C of the ocean, atmosphere, and biosphere [*Walker and Kasting*, 1992]. However, the wide range in CIEs recorded across the PETM lies far beyond that simulated in basic geochemical models [*Dickens*, 2000]. This raises two related questions [*Bowen et al.*, 2004; *Diefendorf et al.*, 2010; *Dickens*, 2011]: (1) What does the range in δ^{13}C mean? (2) What is the correct value for the change in the δ^{13}C of the entire exogenic carbon pool? Clearly, modeling a 2‰ or a 7‰ CIE in the exogenic carbon cycle makes an enormous difference to understanding causes and effects of a massive carbon input [*Dickens et al.*, 1997; *Pagani et al.*, 2006a; *Zeebe et al.*, 2009; *Cui et al.*, 2011].

[10] Other hyperthermal events of the early Paleogene have received far less attention than the PETM, in part because they were discovered relatively recently. Nonetheless, it is already clear that similar issues regarding δ^{13}C records manifest for these events. For example, about 10 δ^{13}C records are presently available across ETM-2 and they show a variance in CIE of 1.4‰–3.8‰ [*Cramer et al.*, 2003; *Lourens et al.*, 2005;

Nicolo et al., 2007; *Sluijs et al.*, 2009; *Stap et al.*, 2009, 2010; *Clementz et al.*, 2011; *Schoon et al.*, 2011; *Abels et al.*, 2012]. This range may increase with additional work using new locations and different substrates, as has been the case for the PETM.

[11] Furthermore, long-term carbon isotope records spanning the early Paleogene may deviate from one another. Planktonic and benthic foraminifer δ^{13}C records from several locations exhibit a ~2‰ decrease from the late Paleocene through the early Eocene (~58–53 Ma; Figure 1) [*Shackleton and Hall*, 1984; *Zachos et al.*, 2001; *Hilting et al.*, 2008]. Within this interval, ~1‰ of the drop occurred between the PETM and ETM2. However, over the same time but in a sediment sequence from the Arctic, there is an ~4‰ decrease in $\delta^{13}C_{TOC}$ (Figure 1) [*Stein et al.*, 2006; *Sluijs et al.*, 2009]. Consequently, individual δ^{13}C records seem to deviate from global exogenic trends on both long and short time scales.

3. Generic Causes

[12] The δ^{13}C of a carbon-bearing phase (substrate) can be related to the δ^{13}C of the exogenic carbon cycle through three basic equations:

$$\delta^{13}C_{SUBSTRATE} = X\% \bullet \delta^{13}C_X + Y\% \bullet \delta^{13}C_Y + Z\% \bullet \delta^{13}C_Z + \ldots \quad (1)$$

$$\delta^{13}C_X = f + \delta^{13}C_{LOCAL} \quad (2)$$

$$\delta^{13}C_{LOCAL} = g + \delta^{13}C_{EXOGENIC} \quad (3)$$

where "substrate" denotes an analyzed carbon-bearing phase (e.g., bulk carbonate), X, Y, Z, etc., denote specific components of a substrate (e.g., foraminiferal and nannofossil carbonate), "local" denotes the carbon pool from which a substrate precipitates (e.g., HCO_3^-), f represents the offset in δ^{13}C between the local pool and the substrate (e.g., fractionation factor [e.g., *Farquhar et al.*, 1989]), and g is the offset in δ^{13}C between the local pool and the average of the global exogenic carbon pool. The third equation ultimately relates to a larger mass balance:

$$\delta^{13}C_{EXOGENIC} = (\delta^{13}C_{LOCAL\text{-}A} \bullet M_{LOCAL\text{-}A} + \delta^{13}C_{LOCAL\text{-}B} \bullet M_{LOCAL\text{-}B} + \ldots)/(M_{EXOGENIC}) \quad (4)$$

where M is mass, A, B, C are different pools of carbon within the exogenic carbon cycle, and $M_{EXOGENIC}$ is the sum of all local carbon reservoirs.

[13] Several factors might cause individual carbon isotope records to vary in shape and magnitude from that of the global exogenic carbon cycle during a carbon cycle perturbation [e.g., *Bowen et al.*, 2004; *Diefendorf et al.*, 2010; *Oehlert et al.*, 2011]. Collectively, there are three general possibilities, which relate to the above equations.

[14] First, most δ^{13}C records comprise mixtures of several carbon sources (equation (1)). For example, bulk marine carbonate records are derived from agglomerations of many nannofossil and foraminifer taxa, and might also include authigenic carbonate; bulk organic carbon records constructed using marine sediments typically represent contributions from marine and terrestrial organic matter, as well as different taxa within the marine and terrestrial realms; higher-plant n-alkane records may be derived from multiple species of gymnosperms, angiosperms and ferns. In many cases, we are unlikely aware of all contributors to the mixture. If the δ^{13}C values of components (X, Y, Z, etc.) within the mixture differ significantly, any change in the relative abundance of the components over time will cause a deviation in δ^{13}C [e.g., *Bralower*, 2002; *Stoll*, 2005; *Schouten et al.*, 2007]. The timing and magnitude of a CIE as recorded in a substrate can thus differ from that of the exogenic carbon pool as the proportion of components changes. This effect can be significant, as discussed below.

[15] An extension of this concept can occur with mixing of material of different age [*Leithold et al.*, 2006]. That is, the components (X, Y, Z, etc.) could represent an identical substrate, but formed at different times, such as before and during a CIE, and subsequently mixed. Bioturbation provides one obvious means for this to occur [*John et al.*, 2008; *Leon-Rodriguez and Dickens*, 2010; *Stap et al.*, 2010]; another is discussed below. In any case, mixing of components of different age would lead to a different expression of the CIE than that of the exogenic carbon cycle. Generally, it should dampen the magnitude by ~1‰ and "smear" the CIE by at least several thousand years [*Stap et al.*, 2010; *Cui et al.*, 2011; *Sluijs et al.*, 2012].

[16] Second, the carbon isotope fractionation between the substrate and the local carbon pool can change (equation (2)). This is because many environmental conditions might change coincident with variations in global carbon cycling. For example, the carbon isotope fractionation between atmospheric CO_2 and organic matter might change in terrestrial plants because of different water use efficiency [e.g., *Bowen et al.*, 2004; *Schouten et al.*, 2007]; the fractionation between DIC and producers of marine calcite might change because of different seawater pH [*Uchikawa and Zeebe*, 2010]. The net result may be an offset between the CIE as recorded in the substrate and the CIE of the local carbon source. Conceivably, such offsets can exceed 1‰–2‰ [*Bowen et al.*, 2004; *Uchikawa and Zeebe*, 2010].

[17] Third, the δ^{13}C of the local carbon pool from which a carbon-bearing phase precipitated could change relative to the exogenic carbon cycle (equation (3)). For example, during the hyperthermals and at the small scale, river inputs to some coastal regions appear to have increased significantly [e.g., *John et al.*, 2008; *Sluijs et al.*, 2008b]. Given the relationship between salinity and the δ^{13}C of dissolved inorganic carbon (DIC) on shelves [*Spiker and Schemel*, 1979; *Chanton and Lewis*, 1999], excess river runoff, would have decreased the local δ^{13}C, so that the negative δ^{13}C excursion in neritic carbonate or organic carbon would be greater than expected. This effect may be significant because the $\delta^{13}C_{DIC}$ of river water is typically approximately 10‰ lower than that of seawater [*Spiker and Schemel*, 1979], and has therefore been invoked as a cause for a −1.5‰ amplification of marine δ^{13}C records on the New Jersey margin across the PETM [*Dickens*, 2011]. Certain organisms may also have changed their habitat, and consequently incorporated C from different parts of the water column. As one possibility, planktonic foraminifera might migrate down in the water during extreme warming [e.g., *Handley et al.*, 2008]. Because of strong $\delta^{13}C_{DIC}$ gradients with depth in many surface ocean regions (e.g., Global Ocean Data Analysis Project data [*Key et al.*, 2004]) the local δ^{13}C would be lower, which would amplify the CIE relative

to that of the exogenic carbon cycle. This provides one means to reconcile the aforementioned 2.5‰ difference in the magnitude of the CIE between thermocline dwelling foraminifera and mixed layer dwelling foraminifera on Maud Rise across the PETM [*Dickens*, 2011].

[18] For constraining changes in the mass and flow of carbon in the exogenic carbon cycle, quantification of changes in *f* and *g* are desirable (equations (2) and (3)). This is because they represent offsets between sedimentary proxy carriers, individual carbon reservoirs, and the global exogenic carbon pool. We suspect that most, if not all, δ^{13}C records across the PETM and other hyperthermals have strong potential for bias. It is highly unlikely that any particular δ^{13}C record shows the true shape and magnitude of the CIE for the global exogenic carbon cycle.

[19] This issue becomes even more problematic (and intriguing) when one considers mass balance (equation (4)). In all likelihood, between 85 and 95% of the exogenic carbon cycle, by mass, has existed as dissolved HCO_3^- in ocean water below the mixed layer throughout the Phanerozoic. This necessarily implies that the δ^{13}C of the deep ocean always dominates the overall δ^{13}C composition of the entire exogenic carbon cycle. Even if δ^{13}C excursions larger than 3.5‰ in magnitude were faithfully recording carbon isotope changes in shallow marine and atmospheric carbon reservoirs, they cannot be used to argue for such changes in the whole exogenic carbon cycle, unless such changes manifest in deep ocean records. Typically, thermocline dwelling and benthic foraminifer δ^{13}C records in open ocean sections across the PETM do not exceed 3‰. Nonetheless, it is important to understand the range in δ^{13}C across substrates during the early Paleogene and tease out the cause behind this variance, because such information may give us crucial insights to past processes during major environmental change.

4. Separating Substrate Effects From $\delta^{13}C_{TOC}$ Records

4.1. Background and Rationale

[20] To explore the conceptual ideas outlined above, we turn to carbon isotope records of total organic carbon ($\delta^{13}C_{TOC}$) in marine sediment. At least 15 such records have now been generated across the PETM, and these show a large range in magnitude for the CIE [e.g., *McInerney and Wing*, 2011]. Some records, such as at Tawanui, New Zealand, show a CIE of ~2‰ [*Kaiho et al.*, 1996; *Crouch et al.*, 2001], some, such as at ODP Site 1172 on the East Tasman Plateau, show a CIE of ~3‰ [*Sluijs et al.*, 2011], while some, such as in the Arctic and in the North Sea, show a CIE exceeding 5‰ [e.g., *Sluijs et al.*, 2006, 2007b; *Cui et al.*, 2011; *Harding et al.*, 2011] (Figure 2). The variation in magnitude of the CIE clearly must reflect factors other than the change in δ^{13}C of the exogenic carbon cycle, or even the atmosphere. Such differences might be attributed to potential hiatuses at the onset of the CIE [e.g., *Hollis et al.*, 2005a; *McCarren et al.*, 2009]. Alternatively, they might reflect variations in the composition of organic matter during the PETM, especially the relative portions of terrestrial and marine organic matter [*Crouch et al.*, 2003; *Sluijs et al.*, 2006].

[21] Marine organic matter (MOM) was much more depleted in ^{13}C over long intervals of the Phanerozoic relative to the Holocene. In their review, *Hayes et al.* [1999] indicated values between −26‰ and −28‰ for Paleocene–Eocene times, compared to approximately −20‰ at present day. The difference likely results from high pCO_2 in past ocean waters, which caused increased fractionation against ^{13}C by the carboxylating enzyme Rubisco [*Freeman and Hayes*, 1992]. By contrast, sedimentary terrestrial organic matter δ^{13}C was only slightly higher during the latest Paleocene to earliest Eocene, with values around −24‰ [*Magioncalda et al.*, 2004; *Domingo et al.*, 2009]. Hence, site-specific variations in the relative supply of terrestrial and marine organic carbon should modify $\delta^{13}C_{TOC}$ records in marine sediment across the hyperthermals.

[22] Sediment records from at least six passive continental margins suggest that global average sea level rose during the PETM [e.g., *Sluijs et al.*, 2008a]. Concomitantly, the supply of sediment from rivers to the shelves, including organic matter, increased at many locations [e.g., *Crouch et al.*, 2003; *Hollis et al.*, 2005b; *Giusberti et al.*, 2007; *Sluijs et al.*, 2008b]. These two processes impact the supply of terrestrial material to a specific continental margin site differently, and wide deviations in the proportion of terrestrial and marine organic matter might be expected during the PETM. In particular, at Tawanui, the percentage of terrestrial palynomorphs increased during the PETM [*Crouch et al.*, 2003]. This was attributed to greater riverine runoff and terrestrial discharge, and was offered as an explanation for why the CIE expressed by $\delta^{13}C_{TOC}$ is relatively small at this location [*Crouch et al.*, 2003]. Can the opposite effect, a greater percentage of marine organic carbon, explain the relatively large CIEs in $\delta^{13}C_{TOC}$ records at locations such as the North Sea and the Arctic Ocean?

[23] The relative proportions of terrestrial and marine organic carbon might be disentangled with measurements of the branched and isoprenoid tetraether (BIT) index. This index describes the relative proportions of specific terrestrial and marine lipds known as glycerol dialkyl glycerol tetraethers (GDGTs); it is defined as [*Hopmans et al.*, 2004]

$$\mathrm{BIT} = [\mathrm{I} + \mathrm{II} + \mathrm{III}]/[\mathrm{I} + \mathrm{II} + \mathrm{III} + \mathrm{IV}]$$

where I, II, and III are terrestrial GDGTs and IV is a marine GDGT. The terrestrial branched GDGTs are produced in soils by bacteria and transported to the ocean by rivers, while the marine isoprenoid GDGT, named crenarcheol, is are dominantly produced in the ocean by planktonic archaea. The exact source of the terrestrial lipids remain unclear [*Sinninghe Damsté et al.*, 2011], and absolute BIT values should be considered with care because interlaboratory comparisons show that analyses are not straightforward [*Schouten et al.*, 2009]. In addition, organic carbon derived from soils may not scale linearly with the total abundance of terrestrial organic matter found in marine sediments [*Weijers et al.*, 2009]. Regardless, the BIT index has emerged as a reliable proxy to quantify the relative amounts of terrestrial and marine organic matter in marine sediments on glacial-interglacial cycles [*Ménot et al.*, 2006] as well as deep time intervals, such as the hyperthermals [*Sluijs et al.*, 2008a, 2011].

[24] The relative portions of terrestrial (pollen and spores) and marine (mostly dinoflagellate cysts) palynomorphs might also serve as a proxy for the relative abundances of terrestrial and marine organic matter. As for the BIT index, this approach

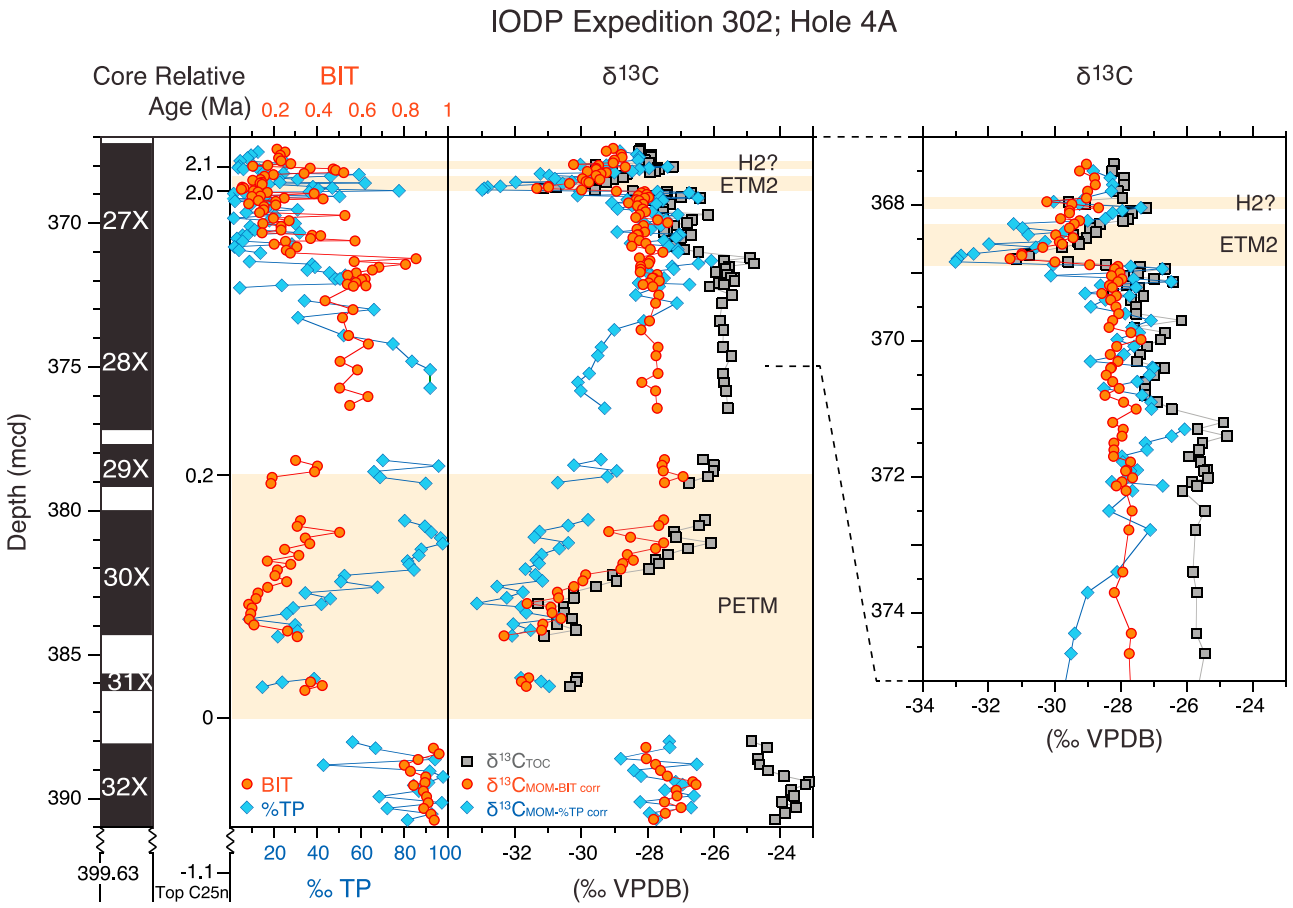

Figure 3. Geochemical and palynological records across the uppermost Paleocene and lower Eocene of IODP Site 4A, Lomonosov Ridge, Arctic Ocean. (left) The δ^{13}C of total organic carbon (TOC) and δ^{13}C of marine organic matter (MOM) reconstructed by subtracting the terrestrial component from the $\delta^{13}C_{TOC}$ values using equations (8) and (9). (right) The BIT index and percentage terrestrial palynomorph (%TP) data used to calculate $\delta^{13}C_{MOM}$. Data are from *Sluijs et al.* [2008b].

has potential problems. In particular, species-specific pollen production and transport processes can affect the relationship between the percentage terrestrial palynomorphs (%TP) and the fraction of terrestrial organic matter in marine sediments.

[25] Importantly, the BIT index and the %TP have different taphonomy, which is the pathway from biological origin to burial in sediment. Rivers can transport both GDGTs and terrestrial palynomorphs to the ocean. Branched GDGTs have not been observed in atmospheric dust [*Hopmans et al.*, 2004]. However, wind can transport terrestrial palynomorphs, particularly saccate pollen of gymnosperm plants. Moreover, the size of the material is much different: GDGTs are nominally a few nm, while terrestrial palynomorphs are typically between five and several tens of μm. Temporal records of the two proxies, when and where consistent, thus likely reflect past delivery of terrestrial organic matter to marine sediments.

4.2. Material and Methods

[26] IODP Expedition 302 drilled Hole 4A on Lomonosov Ridge, central Arctic Ocean in 2004 (Figure 2) [*Backman et al.*, 2006]. Uppermost Paleocene–lowermost Eocene sediments in this hole (Cores 32X – 27X) were deposited at ~85°N, and likely on the continental shelf [*O'Regan et al.*, 2008], as indicated by generally high abundances of terrestrial components, including plant remains and abundant river-transported pollen and spores and terrestrial biomarkers [e.g., *Sluijs et al.*, 2008b]. The section lacks biogenic carbonate suitable for carbon isotope stratigraphy. However, both the PETM and ETM2 have been identified based on biostratigraphy and prominent CIEs in various organic components [*Pagani et al.*, 2006b]. Across the PETM, a large magnitude CIE of ~6‰ appears in bulk organic carbon isotope records (Figure 1) [*Sluijs et al.*, 2006] and angiosperm-specific biomarkers yield a CIE of ~7‰ [*Schouten et al.*, 2007]. However, the CIE is muted in other phases at this location, being 4.5‰–5‰ in leaf wax n-alkanes [*Pagani et al.*, 2006b], and about 3‰ in gymnosperm specific biomarkers [*Schouten et al.*, 2007]. Clearly, various records at this site are affected by changes in the composition of the organic substrate (equation (1)).

[27] Records of $\delta^{13}C_{TOC}$, BIT and palynomorphs have been generated on 123 samples at Hole 302-4A that span the latest Paleocene and earliest Eocene (Figure 3) [*Sluijs et al.*, 2008b]. The $\delta^{13}C_{TOC}$ records mark the negative CIEs associated with the PETM and ETM2 as well as a general

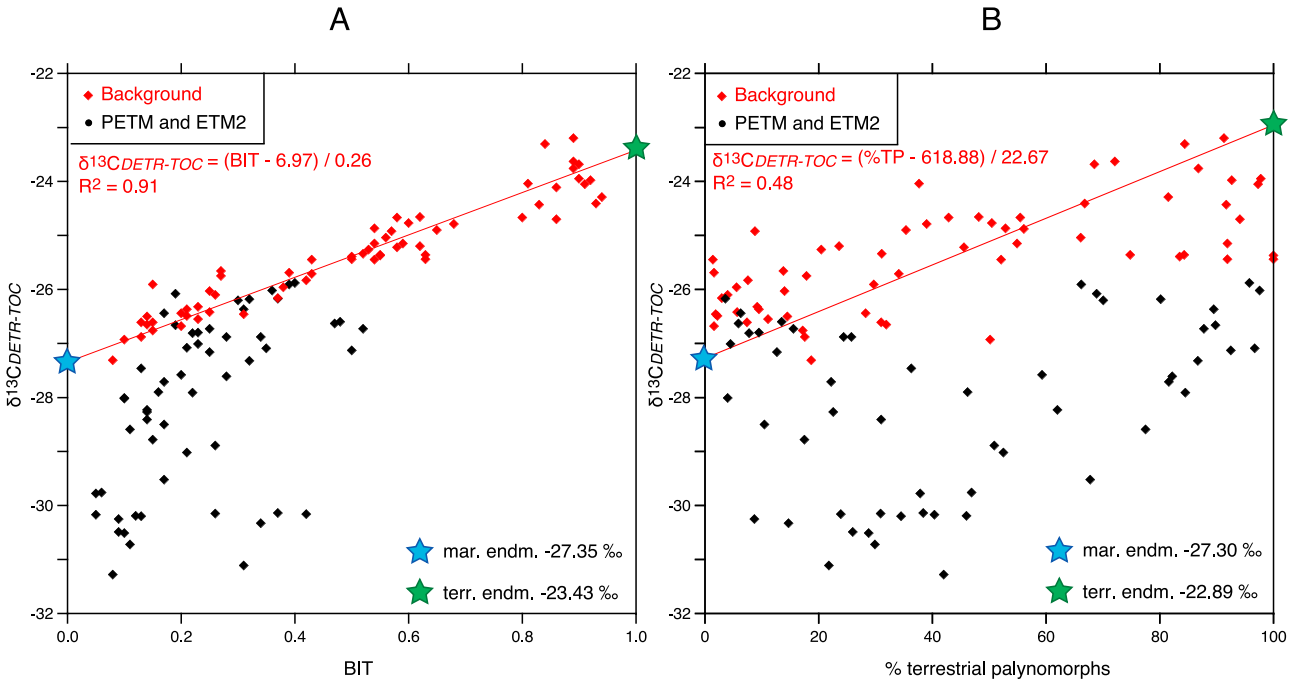

Figure 4. X-Y plot between $\delta^{13}C_{TOC}$ (detrended for the long-term exogenic trend; see section 4.2) and (a) BIT index and (b) percentage terrestrial palynomorphs (%TP) at IODP Site 4A, Lomonosov Ridge, Arctic Ocean. Black data points represent samples from the PETM or ETM2. Correlations are calculated based on the samples from outside of these hyperthermals (Background), which are the red data points. Data are from *Sluijs et al.* [2008b].

decrease across the entire interval. These trends are generally mimicked by the BIT index and the percentage terrestrial palynomorphs (%TP) records, which show that the contribution of terrestrial organic matter varies significantly across the hyperthermals, and also over the long-term late Paleocene to early Eocene. This enables us to assess the relation between $\delta^{13}C_{TOC}$ and organic matter origin. Moreover, this relation can be used to calculate the $\delta^{13}C$ of the marine and terrestrial organic matter end-members. Ultimately, we use this result to correct $\delta^{13}C_{TOC}$ records of the hyperthermals for the effect of changing contribution of marine and terrestrial organic carbon.

[28] To quantify the relation between organic matter origin and $\delta^{13}C_{TOC}$, exogenic trends must be excluded (equation (3)). Bulk carbonate, as well as surface, thermocline and deep ocean foraminifer $\delta^{13}C$ records show a gradual decrease by ~2‰ in several ocean basins during the late Paleocene to early Eocene (59–51 Ma) [*Shackleton and Hall*, 1984; *Zachos et al.*, 2001; *Hilting et al.*, 2008]. Within this trend, the interval from just before the PETM to just after ETM2 (~56–54 M), yields a ~1‰ negative shift (Figure 1). Because the same trend is seen in surface, intermediate and deep ocean records, we consider this value to be close to the global exogenic $\delta^{13}C$ trend. To correct for this effect, we detrend the $\delta^{13}C_{TOC}$ data ($\delta^{13}C_{DETR\text{-}TOC}$) using the available age model [*Sluijs et al.*, 2008b], using uppermost Paleocene values as the anchor point (Figure 1). Subsequently, we apply linear regression analyses to quantify the relation between $\delta^{13}C_{TOC}$ and two proxies for the relative amount of terrestrial organic matter in uppermost Paleocene–lower Eocene sediments, BIT index and percent terrestrial palynomorphs of the total palynomorphs sum >15 μm (%TP).

4.3. Results and Discussion

[29] The collective data at Hole 302-4A show some important relationships. For samples "outside" the hyperthermal intervals, a strong linear relationship ($R^2 = 0.91$) exists between the $\delta^{13}C_{TOC}$ and the BIT index (Figure 4). This implies that varying proportions of terrestrial and marine organic matter impact the $\delta^{13}C_{TOC}$ record throughout the studied interval.

[30] The correlation between $\delta^{13}C_{TOC}$ and the percentage of terrestrial palynomorphs (%TP) is less strong ($R^2 = 0.48$). This could mean that taphonomic processes, particularly transport from the continent into the marine basin, have blurred the correlation between $\delta^{13}C_{TOC}$ and %TP. Indeed, bottom water energies across the late Paleocene–early Eocene interval at the ACEX drill site fluctuated considerably [*Martinez et al.*, 2009; *März et al.*, 2010], which might have differently affected BIT and %TP. In addition, transport of freshwater from the hinterland into the marine system might have (seasonally) increased due to changing precipitation patterns [*Pagani et al.*, 2006b], which likely affected taphonomy of the various organic components differently.

[31] Selective preservation probably does not explain the marked differences in the organic biomarker and palynomorph assemblages [*Sluijs et al.*, 2006]. First, the preservation of organic matter is also excellent outside the hyperthermals due to consistently low oxygen concentrations on the seafloor throughout the late Paleocene to early Eocene [*Stein et al.*, 2006; *Sluijs et al.*, 2008b]. Second, BIT and %TP compare the relative abundance of structurally similar organic components that are equally susceptible to oxidation. We tested for a relation between $\delta^{13}C_{TOC}$ and %TOC for the same samples to

Table 1. Calculated Marine and Terrestrial Organic Matter δ^{13}C End-Members and the Calculated Magnitudes of the CIEs Across the PETM, ETM2 and H2 in Marine Organic Matter

	Marine δ^{13}C End-Member	Terrestrial δ^{13}C End-Member	$\delta^{13}C_{TOC}$ Dependence of Terrestrial Organic Matter	CIE PETM	CIE ETM2	CIE ?H2?
Percentage terrestrial palynomorph correction	−27.30	−22.89	0.044‰/%TP	−3.86	−4.55	−0.93
BIT index correction	−27.35	−23.43	3.922‰/BIT-unit	−3.49	−2.60	−0.49
TOC				−5.87	−3.38	−1.51

further investigate a potential impact of preservation but we found no significant relationship ($R^2 < 0.1$).

4.3.1. The δ^{13}C of Terrestrial Organic Matter ($\delta^{13}C_{TER}$)

[32] The empirical linear relationships between $\delta^{13}C_{DETR\text{-}TOC}$ and BIT or %TP (Figure 4) are described as follows:

$$\delta^{13}C_{DETR\text{-}TOC} = (BIT - 6.97)/0.26 \quad (5)$$

$$\delta^{13}C_{DETR\text{-}TOC} = (\%TP - 618.88)/22.67 \quad (6)$$

In these equations, the pure terrestrial end-member has BIT = 1 and %TP = 100. This implies that bulk terrestrial organic carbon has a δ^{13}C of −23.4‰ according to the BIT equation, and −22.9‰ according to the %TP equation (Table 1).

[33] A compilation of published $\delta^{13}C_{TOC}$ data (Figure 5) allows for comparison on an interregional scale. The $\delta^{13}C_{TOC}$ in terrestrial early Paleogene sequences (per definition $\delta^{13}C_{TER}$) from multiple continental locations exhibit average values between −23‰ and −25‰ [*Collinson et al.*, 2003; *Carvajal-Ortiz et al.*, 2009; *Domingo et al.*, 2009]. The calculated Arctic terrestrial end-member value is relatively high, but reasonably close to time-equivalent terrestrial deposits elsewhere, despite significant differences in vegetation, sedimentary conditions and preservation.

4.3.2. The δ^{13}C of Marine Organic Matter ($\delta^{13}C_{MOM}$)

[34] Equations (5) and (6) also define a marine end-member, when BIT and %TP are set to zero. For samples exclusive of the hyperthermals, $\delta^{13}C_{MOM}$ is approximately −27.3‰ using either the BIT or %TP equation (Table 1). This value is consistent with other δ^{13}C measurements of Paleocene–Eocene marine organic carbon [*Hayes et al.*, 1999]. Early Paleogene $\delta^{13}C_{MOM}$ was approximately 7‰ lower than Holocene marine organic matter. This was the case despite higher sea surface temperatures in the Arctic Ocean [*Sluijs et al.*, 2006] and elsewhere [*Zachos et al.*, 2008], which should increase $\delta^{13}C_{MOM}$ values relative to present day due to temperature-dependent thermodynamic isotopic fractionation [e.g., *Gruber et al.*, 1999]. However, an early Paleogene $\delta^{13}C_{MOM}$ of −27.3‰ is consistent with significantly higher past pCO_2, which, as noted previously, should result in increased ^{13}C discrimination during carbon fixation [*Freeman and Hayes*, 1992].

4.3.3. Calculating $\delta^{13}C_{MOM}$ From $\delta^{13}C_{TOC}$

[35] Changes in substrate composition are a major potential cause for differences in δ^{13}C responses during hyperthermals (equation (1)). The correlations between $\delta^{13}C_{DETR\text{-}TOC}$ and terrestrial components (Figure 4; equations (5) and (6)) allow corrections of each $\delta^{13}C_{TOC}$ value at Hole 302-4A, including those within the hyperthermals. These corrections account for the influence of different proportions of marine and terrestrial organic carbon upon $\delta^{13}C_{TOC}$, and can be expressed as "dependences" using BIT or %TP (Table 1):

$$\begin{aligned}\text{Dependence (BIT)} &= \left(\left(\delta^{13}C_{TER}\right) - \left(\delta^{13}C_{MOM}\right)\right)/1 \\ &= (-23.42 + 27.35)/1 \\ &= 3.922‰/\text{BIT unit}\end{aligned} \quad (7)$$

$$\begin{aligned}\text{Dependence (\%TP)} &= \left(\left(\delta^{13}C_{TER}\right) - \left(\delta^{13}C_{MOM}\right)\right)/100 \\ &= (-22.89 + 27.30)/100 \\ &= 0.044‰/\%TP\end{aligned} \quad (8)$$

Following equations (5) and (6), the terrestrial organic matter contributions to $\delta^{13}C_{TOC}$ of each sample can now be "removed," leading to equations to calculate $\delta^{13}C_{MOM}$:

$$\begin{aligned}\delta^{13}C_{MOM} &= \delta^{13}C_{TOC} - \text{Dependence (BIT)} \bullet \text{BIT} \\ &= \delta^{13}C_{TOC} - 3.922 \bullet \text{BIT}\end{aligned} \quad (9)$$

$$\begin{aligned}\delta^{13}C_{MOM} &= \delta^{13}C_{TOC} - \text{Dependence (\%TP)} \bullet \%TP \\ &= \delta^{13}C_{TOC} - 0.044 \bullet \%TP\end{aligned} \quad (10)$$

[36] A long-term 4‰ decline in $\delta^{13}C_{TOC}$ from approximately −24‰ to −28‰ occurred at Hole 302-4A between the upper Paleocene (circa 56 Ma) and the lower Eocene (circa 53 Ma; Figure 3). The magnitude of this shift is reduced to ~2‰ in calculated $\delta^{13}C_{MOM}$ curves (Figure 3). This implies that the long-term (>3 Myr) decrease in the contribution of terrestrial organic matter to the depositional location, has affected the $\delta^{13}C_{TOC}$ signal. As discussed above, another ~1‰ of the bulk $\delta^{13}C_{TOC}$ signal can be explained by a change in the exogenic carbon cycle; such a drop has been observed in multiple marine calcite δ^{13}C records (Figure 1) [*Shackleton and Hall*, 1984; *Zachos et al.*, 2001; *Hilting et al.*, 2008]. The residual ~1‰ shift in the long-term $\delta^{13}C_{MOM}$ curve, from approximately −27‰ to −28‰, suggests a decrease in $\delta^{13}C_{MOM}$ at this location, independent of changes in basic composition or the δ^{13}C of the global exogenic carbon cycle. One possibility would be a change in the δ^{13}C of local DIC pool relative to that of the exogenic carbon cycle (equation (3)). The BIT index and %TP decrease significantly over the long-term, consistent with a reduced supply of terrestrial organic carbon. One explanation for this pattern is greater distance to shore [*Sluijs et al.*, 2009], because Lomonosov Ridge was rifting away from the Eurasian shelf during the early Paleogene [*O'Regan et al.*, 2008]. However, given the relationship

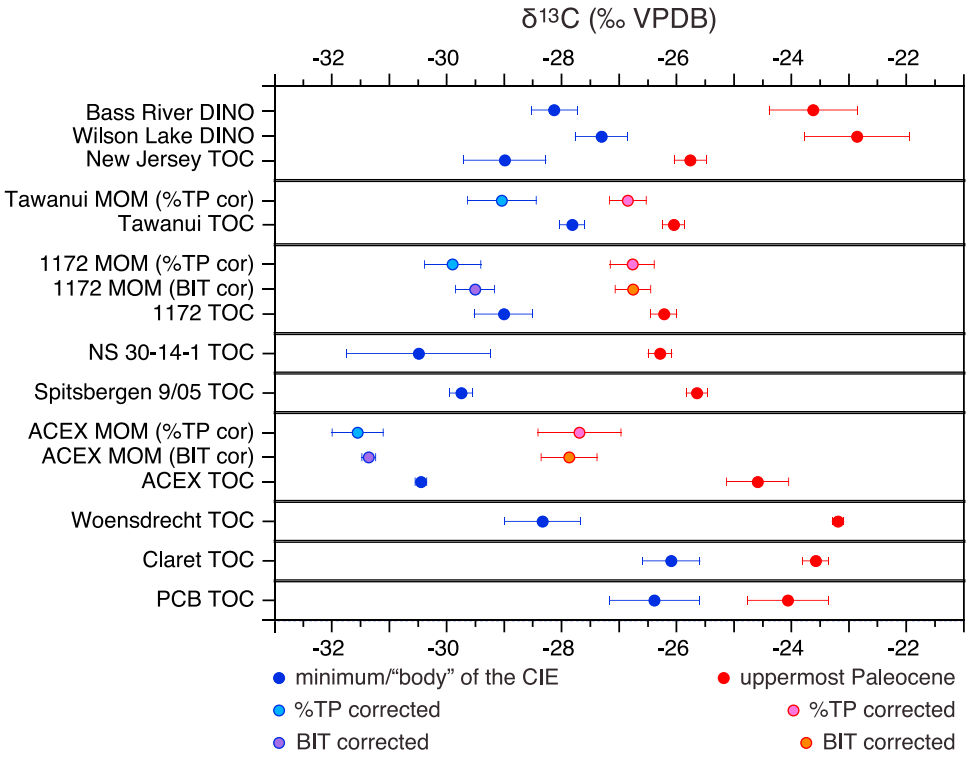

Figure 5. Compilation of published organic carbon δ^{13}C data across a virtual transect of outer shelf (top) to terrestrial (bottom) sites. Data points reflect averaged (with standard deviation error) upper Paleocene values in red, pink, and yellow and averaged early PETM values in blues and purple. Dark blue and red are $\delta^{13}C_{TOC}$ values, and pink and orange reflect $\delta^{13}C_{MOM}$ values as calculated using %TP and BIT index, respectively. Shown are dinoflagellate cyst (DINO) δ^{13}C data [*Sluijs et al.*, 2007b] and $\delta^{13}C_{TOC}$ data from the New Jersey Shelf [*Kopp et al.*, 2009]; Tawanui, New Zealand [*Kaiho et al.*, 1996]; ODP Site 1172, East Tasman Plateau [*Sluijs et al.*, 2011]; North Sea Site 30/14–1 [*Sluijs et al.*, 2007b]; Spitsbergen Core 9/05 [*Cui et al.*, 2011]; IODP Site 4A (Arctic Coring Expedition, ACEX) [*Sluijs et al.*, 2006]; Woensdrecht, Netherlands [*Sluijs et al.*, 2008a]; Claret, Spain [*Domingo et al.*, 2009]; and the Polecat Bench (PCB) Section in the Bighorn Basin, Wyoming [*Magioncalda et al.*, 2004].

between δ^{13}C of DIC and coastal proximity [*Spiker and Schemel*, 1979; *Chanton and Lewis*, 1999], this effect should have increased Arctic $\delta^{13}C_{MOM}$, opposite to the record (Figure 3). A more satisfactory explanation is a change in the fractionation between marine MOM and the local DIC pool (equation (2)). In particular, there was a significant increase in pCO_2 between 56 Ma and 53 Ma. This would be consistent with a concomitant long-term drop in the depth of the calcite compensation depth over the same time interval [*Hancock et al.*, 2007; *Leon-Rodriguez and Dickens*, 2010].

[37] As with the long-term trends, the $\delta^{13}C_{MOM}$ and $\delta^{13}C_{TOC}$ records display significant temporal differences relative to each other across the hyperthermals (Figure 3). The $\delta^{13}C_{MOM}$ decreased from −27.5‰ to −28‰ during the uppermost Paleocene to −31‰ to −31.5‰ during the start of the PETM, using either the %TP or BIT correction (Table 1). The magnitude of the CIE is therefore −3.5‰ to −4‰ in marine organic carbon, compared to nearly −6‰ in TOC. The simplest explanation is that the proportion of marine organic carbon increased on Lomonosov Ridge during the event, as expected for a rise in sea level and as recorded by drops in BIT and %TP values, exaggerating the CIE in $\delta^{13}C_{TOC}$.

[38] Across the onset of ETM2, the $\delta^{13}C_{MOM}$, as calculated using BIT, decreased from approximately −28.2‰ to −30.8‰, implying a CIE of −2.6‰ (Figure 3). By contrast, the CIE in $\delta^{13}C_{TOC}$ is approximately −3.4‰. Again, ETM2 corresponds to a decrease in BIT, and the CIE in $\delta^{13}C_{MOM}$ is probably smaller than in $\delta^{13}C_{TOC}$ because of less terrestrial organic matter. Interestingly, however, the excursion in %TP-corrected $\delta^{13}C_{MOM}$ is extremely large (−4.5‰), because of an increase in the relative abundance of terrestrial palynomorphs (Figure 3). The discrepancy between BIT and %TP may reflect differences in the transport of soil biomarkers and pollen into the basin (see section 4.1). In addition, the R^2 value between $\delta^{13}C_{TOC}$ and %TP is only 0.5 implying a much larger uncertainty in the corrected magnitude of the CIE than using BIT. Because of the much higher R^2, we consider the BIT-corrected estimates of $\delta^{13}C_{MOM}$ to be a more reliable proxy for terrestrial organic matter input than the %TP correction.

[39] The H2 event occurred ~100 ka after ETM2 [*Cramer et al.*, 2003; *Lourens et al.*, 2005] and represents a hyperthermal with a relatively small negative CIE [*Stap et al.*, 2010]. Based on a ~1.5‰ negative CIE in $\delta^{13}C_{TOC}$, the H2 event appears to occur in Hole 302-4A approximately 80 cm above the onset of ETM2 [*Sluijs et al.*, 2009] (Figure 3). However, marine biomarkers of primary producers, such as phytane, highly branched isoprenoid (HBI) alkenes from specific diatom genera and several hopanoids from

cyanobacteria do not show a negative CIE across H2 in these sediments [*Schoon et al.*, 2011]. The H2 CIE was potentially masked because of an increase in primary production [*Schoon et al.*, 2011], which would cause a local increase in $\delta^{13}C_{DIC}$ and hence $\delta^{13}C_{MOM}$ (equation (3)). Alternatively, the CIE as recorded in $\delta^{13}C_{TOC}$, does not reflect H2 at all but rather a change in the relative contributions of various sources of organic matter (equation (1)) [*Schoon et al.*, 2011]. The $\delta^{13}C_{MOM}$ curves, however, show excursions of −0.5‰ and −0.9‰ following the BIT and %TP corrections, respectively. This CIE could reflect H2 and is, in fact, close to the reconstructed magnitude of the excursion in the deep ocean as recorded in benthic foraminifera (−0.8‰ [*Stap et al.*, 2010]).

[40] How do the above estimates of the magnitude of the CIEs of the PETM and ETM2 in marine organic matter compare to estimates from the largest reservoir in the exogenic carbon pool, the deep sea? Proxy carriers from deep sea benthic foraminifera typically record a CIE of 2‰ to 3‰ for the PETM [*McInerney and Wing*, 2011], although one record shows a relatively large 3.5‰ CIE [*McCarren et al.*, 2009]. The latter record is from a relatively shallow deep ocean section and may stratigraphically complete because it was less affected by carbonate dissolution. The 3.5‰–4‰ CIE we find in $\delta^{13}C_{MOM}$ is similar to or slightly larger than that recorded in deep sea benthic foraminifera. The CIE as recorded in single species deep ocean benthic foraminifera is approximately −1.4‰ across the onset of ETM2 [*Stap et al.*, 2010]. Hence, similar to the PETM, the CIE as reflected in Arctic $\delta^{13}C_{MOM}$ is exaggerated by ∼1‰ using the BIT correction, and ∼3‰ using the %TP correction.

[41] Because the patterns of climate change during the PETM and ETM2 in the Arctic [*Sluijs et al.*, 2009], and therefore the potential forcing factors for offsets between $\delta^{13}C_{MOM}$ excursions and global exogenic trends, are similar, the potential explanations for the large CIE in $\delta^{13}C_{MOM}$ across ETM2 are the same. Even ignoring global mass balance considerations (equation (4)), there are several issues. First, our corrections only partly address changes in substrate composition (equation (1)). Changes in marine biota, which evidently occurred during both the PETM and ETM2 [*Sluijs et al.*, 2008b, 2009], may have changed the relative proportions of different marine organic carbon components that contributed to total MOM. In any case, three effects should have accentuated the CIEs as recorded in Arctic marine organic matter relative to the CIEs of the entire exogenic carbon pool: (1) A rise in pCO_2 would have increased carbon isotope fractionation by marine primary producers (equation (2)). Moreover, an increase in organic matter input (2) and river water supply (3) to the Arctic Ocean would have contributed to decreasing $\delta^{13}C_{DIC}$ (equation (3)) [*Spiker and Schemel*, 1979; *Chanton and Lewis*, 1999; *Fry*, 2002]. This implies that the −3.5‰ to −4‰ shift in $\delta^{13}C_{MOM}$ is likely exaggerated relative to the magnitude of the CIE of the global exogenic carbon pool.

4.3.4. Comparison to Other $\delta^{13}C_{TOC}$ Records

[42] The $\delta^{13}C_{TOC}$ records at Hole 302-4A appear impacted by significant mixing of terrestrial and marine organic carbon with different $\delta^{13}C$. Presumably, such mixing would affect other $\delta^{13}C_{TOC}$ records in marine sediments emplaced on early Paleogene continental margins, and this seems to be the case (Figure 5). Similar to Hole 302-4A, records from locations deposited close to the paleoshoreline, such as at Woensdrecht (North Sea) [*Sluijs et al.*, 2008a] have relatively high $\delta^{13}C_{TOC}$ values (approximately −23‰ outside the hyperthermals) for late Paleocene–early Eocene sediment. Indeed, $\delta^{13}C_{TOC}$ values at these locations are close to those of $\delta^{13}C_{TER}$ in continental sections at Claret (Spain, −23‰ to −24‰ [*Domingo et al.*, 2009]) and at Polecat Bench (Wyoming, −23‰ to −25‰ [*Magioncalda et al.*, 2004]). By contrast, sediment sections that accumulated further offshore during this time, such as at Site 30–14/1 (central North Sea [*Sluijs et al.*, 2007b]) or at Ocean Drilling Program Site 1172 (East Tasman Plateau [*Sluijs et al.*, 2011]), have intermediate $\delta^{13}C_{TOC}$ values (approximately −26‰, Figure 5) suggestive of greater proportions of marine organic carbon.

[43] Several marine sequences with $\delta^{13}C_{TOC}$ records have additional data that can be used to address marine and terrestrial contributions, as we have outlined for Hole 302-4A. At Site 1172, BIT and palynomorph assemblages have been determined for upper Paleocene and lower Eocene sediment; these records suggest significant sedimentary contributions from both terrestrial and marine sources [*Sluijs et al.*, 2011]. The evolution of $\delta^{13}C_{MOM}$ can be assessed using the $\delta^{13}C_{TOC}$ record, the BIT index and equation (9), which describes the relation between these variables at Hole 302-4A in the Arctic Ocean. Such correction lowers upper Paleocene $\delta^{13}C_{MOM}$ to −26.7‰, very close to the Arctic value and the estimates of *Hayes et al.* [1999] (Figure 5).

[44] Unlike at Hole 302-4A or Site 1172, $\delta^{13}C_{TOC}$ values at Tawanui (New Zealand) are relatively high (−26.1‰) in upper Paleocene sediment, and show a small ∼1.7‰ CIE across the PETM [*Kaiho et al.*, 1996] (Figure 5). Also different: the PETM is marked by a significant increase in %TP, interpreted as reflecting greater riverine discharge [*Crouch et al.*, 2003]. Correction of the $\delta^{13}C_{TOC}$ record for %TP (equation (8) from Hole 4A) results in upper Paleocene $\delta^{13}C_{MOM}$ values of −26.9‰, again close to that estimated for Hole 4A. However, such a correction means that the CIE magnitude across the PETM is greater in $\delta^{13}C_{MOM}$ (−2.1‰). Thus, opposite to Hole 4A and Site 1172, an increase in terrestrial material damped the magnitude of the CIE recorded by bulk organic carbon.

[45] The similarity in estimated $\delta^{13}C_{MOM}$ values between early Paleogene records (pink and orange points in Figure 5) [*Hayes et al.*, 1999] is remarkable considering the variability in $\delta^{13}C_{MOM}$ exhibited in the modern ocean [*Goericke and Fry*, 1994; *Gruber et al.*, 1999]. For the late Paleocene, the Arctic Ocean $\delta^{13}C_{MOM}$ value of −27.3‰ is only slightly lower than the $\delta^{13}C_{MOM}$ records at other sites deposited at lower latitudes (Figure 5). Marine organic matter formed in modern oceans at high latitudes is generally depleted in ^{13}C ($\delta^{13}C_{MOM}$ = between −19‰ and −26‰) relative to that formed at lower latitudes ($\delta^{13}C_{MOM}$ = between −18‰ and −22‰) [*Goericke and Fry*, 1994]. This is generally explained by higher concentrations of dissolved CO_2 in cold polar waters and large seasonal shifts in nutrient availability, which together lead to higher fractionation [*Rau et al.*, 1989; *Freeman and Hayes*, 1992; *Freeman*, 2001]. The intriguing similarity of early Paleogene $^{13}C_{MOM}$ values across latitudes may reflect past ocean conditions, specifically three key differences: (1) the meridional temperature gradient was almost assuredly much smaller [e.g., *Bijl et al.*, 2009; *Huber and Caballero*, 2011], (2) Arctic Ocean

productivity was likely higher [*Knies et al.*, 2008], and (3) ocean DIC concentrations were probably much higher [*Panchuk et al.*, 2008; *Zeebe et al.*, 2009]. All three factors would reduce global $\delta^{13}C_{MOM}$ variability.

[46] Several substrates of organic matter were analyzed for δ^{13}C across the upper Paleocene to lower Eocene deposits on the New Jersey Shelf. Uppermost Paleocene $\delta^{13}C_{TOC}$ from a compilation of sites averages −25.8‰ (Figure 5) [*Kopp et al.*, 2009], likely representing a mixture between dominant marine and some terrestrial organic matter. Surprisingly, two δ^{13}C records of marine organic microfossils, dinoflagellate cysts from the New Jersey Shelf [*Sluijs et al.*, 2007b] show very high upper Paleocene values, close to the terrestrial end-member. Dinoflagellates often occur in intense blooms that may deplete the DIC pool and raise pH [*Hansen*, 2002] to the extent that seawater DIC becomes very rich in ^{13}C. Alternatively, many dinoflagellates take up both HCO_3^- and CO_2 for photosynthesis and several taxa dominantly acquire HCO_3^- [*Rost et al.*, 2006]. The δ^{13}C of HCO_3^- is about 9‰ higher than that of dissolved CO_2 [*Mook et al.*, 1974; *Zeebe and Wolf-Gladrow*, 2001]. These may be important mechanisms leading to high dinocyst δ^{13}C values.

5. Broader Implications

[47] In principle, and for any substrate through any time interval, interpretations of δ^{13}C records in regards to global carbon cycling are subject to three parameters: (1) the abundance of constituent end-members, (2) carbon isotope fractionation relative to the local source of carbon, and (3) the offset in carbon isotope composition between the local carbon source and the exogenic carbon cycle (equations (1)–(3)). Under steady state conditions, individual records may very well provide quantitatively precise information on exogenic carbon cycling. However, when environmental conditions change in the time domain, and these changes impact relationships between "carbon isotope recorders" and the exogenic carbon cycle, interpretations become complicated and intriguing. This particularly holds for episodes of extreme environmental change and major perturbations in global carbon cycling, such as the PETM and other early Paleogene hyperthermals. Multiple factors should have impacted δ^{13}C records differently; this applies to records constructed using different substrates, those constructed at different locations, or both.

[48] For example, *Cui et al.* [2011] measured a −4.2‰ CIE in bulk TOC across the PETM in a marginal marine sequence in Spitsbergen, and suggested that this change represents that within the entire exogenic carbon cycle. First, it remains difficult to support this inference from a mass balance perspective (equation (4)), as no δ^{13}C record from a deep ocean substrate, where the lion's share of carbon lies, shows such a shift [*McInerney and Wing*, 2011]. Second, and more directly, the inference hinges on the notion that the composition of organic matter did not change within the PETM (equation (1)) [*Cui et al.*, 2011]. In fact, the sedimentary organic matter C/N ratios at the studied location vary between 9 and 15. Moreover, the relative abundance of terrestrial and marine palynomorphs at a nearby section [*Harding et al.*, 2011] suggest that the deposition of marine material increased across the PETM at sites on Spitsbergen. Moreover, even if the proportion of terrestrial and marine organic matter did not change at Spitsbergen during the PETM, vegetation may have changed significantly, so that more angiosperms contributed to the terrestrial fraction [*Schouten et al.*, 2007]. In addition, carbon isotope fractionation relative to the local source of carbon has to be assumed constant (equation (2)). For multiple reasons, the measured −4.2‰ CIE in $\delta^{13}C_{TOC}$ at Spitsbergen is probably greater than the magnitude of the CIE excursion for the exogenic carbon cycle, as has been inferred above for Hole 302-4A and other locations (Figure 5).

[49] The magnitude of truly global CIEs, such as those related to the PETM and ETM2 relates to the size of the carbon injection as recorded in sedimentary components [*Dickens*, 2001]. Some authors have suggested that the CIE across the hyperthermals must be very large, because the magnitude of warming is very large [*Kurtz et al.*, 2003; *Higgins and Schrag*, 2006; *Pagani et al.*, 2006a]. This is true, even if the source of carbon is very depleted in ^{13}C source, such as methane, requires a large excursion [*Dickens et al.*, 1997]. The basic assumption underlying this logic, however, is that the injection of ^{13}C-depleted carbon caused all of the warming, while high-resolution records suggest that the onset of warming preceded the CIE [e.g., *Thomas et al.*, 2002; *Sluijs et al.*, 2007b].

[50] Quantification of the magnitudes of CIEs across the PETM and other hyperthermals remains a major challenge at least in terms of the exogenic carbon cycle. Until the generalities of equations (1), (2), (3), and (4) can be constrained in multiple records, the CIEs remain insufficiently constrained. Certainly, however, we argue that smaller CIEs are easier to explain from a mass balance perspective. Moreover, many processes will amplify the magnitude of the CIE during a short-term warming event, certainly in nearshore regions and organic matter substrates.

6. Conclusions

[51] Records of δ^{13}C on various carbon-bearing phases in sediment sections deposited during late Paleocene–early Eocene hyperthermals show a very large variation in the magnitude of their CIEs. The variation depends on location and analyzed substrate. Three factors might cause individual carbon isotope records across the same stratigraphic interval to differ in shape and magnitude from variations in the global exogenic carbon cycle: (1) changes in the relative abundance of components with different δ^{13}C within a measured substrate, (2) changes in isotope fractionation through physiological response to ecological change, and (3) changes in the isotope composition of the carbon source that is fixed. All three factors, which we describe in three simple equations, likely influence many early Paleogene δ^{13}C records, especially across the PETM and other hyperthermal events.

[52] We apply these concepts to records of a late Paleocene–early Eocene interval (~58–52 Ma) from Lomonosov Ridge, Arctic Ocean. Linear regression analyses show correlations between δ^{13}C of total organic carbon (TOC), and two proxies for the relative contribution of terrestrial organic components to TOC: BIT index and palynomorphs. The BIT index, a biomarker-based proxy, correlates to $\delta^{13}C_{TOC}$ with $R^2 = 0.91$, while the abundance of terrestrial pollen and spores shows a weaker correlation with $R^2 = 0.48$. The larger scatter in the %

TP regression is likely do to variations in taphonomy. End-member terrestrial and marine organic matter δ^{13}C values equal approximately −23‰ and −27‰, respectively, which is consistent with published records.

[53] We use these correlations between BIT, %TP and $\delta^{13}C_{TOC}$ to subtract the terrestrial component from the $\delta^{13}C_{TOC}$ record and subsequently calculate the evolution of Arctic marine organic carbon δ^{13}C. The results show that the magnitude of the CIE in $\delta^{13}C_{TOC}$ across the Paleocene-Eocene thermal maximum (PETM) is exaggerated relative to the magnitude of the CIE in marine organic matter by ∼3‰ due to increased contributions of terrestrial organic carbon during the event. Collectively, most, if not all, carbon isotope records across the PETM and likely all major climate perturbations are biased through one or more of the above factors. In fact, this carbon cycle recording problem is universal for all carbon cycle – climate perturbations in Earth's history, including Paleozoic carbon isotope excursions, the Permian–Triassic transition, the Triassic–Jurassic boundary, Mesozoic anoxic events, and the Cretaceous–Paleogene boundary. Indeed, it is highly unlikely that any δ^{13}C record shows the true shape and magnitude of the CIE for the global exogenic carbon cycle. This work introduces a way forward, based on three simple equations and empirically based exclusions of sedimentary components, to improve our quantification of global exogenic carbon cycle trends.

[54] **Acknowledgments.** This research used samples and data provided by the Integrated Ocean Drilling Program (IODP). We thank Christian März and John Higgins for their thorough and constructive reviews, which led to significant improvements of the paper. The European Research Council under the European Community's Seventh Framework Program provided funding for this work by ERC Starting Grant 259627 to A.S. A.S. thanks the Royal Netherlands Academy of Arts and Sciences (KNAW) for a Visiting Professors Programme grant for Dickens.

References

Abdul Aziz, H., F. J. Hilgen, G. M. van Luijk, A. Sluijs, M. J. Kraus, J. M. Pares, and P. D. Gingerich (2008), Astronomical climate control on paleosol stacking patterns in the upper Paleocene–lower Eocene Willwood Formation, Bighorn Basin, Wyoming, *Geology*, *36*(7), 531–534, doi:10.1130/G24734A.24731.

Abels, H. A., W. C. Clyde, P. D. Gingerich, F. J. Hilgen, H. C. Fricke, G. J. Bowen, and L. J. Lourens (2012), Terrestrial carbon isotope excursions and biotic change during Palaeogene hyperthermals, *Nat. Geosci.*, *5*, 326–329, doi:10.1038/ngeo1427.

Adams, C. G., D. E. Lee, and B. R. Rosen (1990), Conflicting isotopic and biotic evidence for tropical sea-surface temperatures during the Tertiary, *Palaeogeogr. Palaeoclimatol. Palaeoecol.*, *77*(3-4), 289–313, doi:10.1016/0031-0182(90)90182-7.

Backman, J., K. Moran, D. B. McInroy, L. A. Mayer, and Expedition 302 Scientists (2006), *Proceedings of the Integrated Ocean Drilling Program*, vol. 302, Integrated Ocean Drill. Program Manage. Int., Edinburgh, UK.

Bains, S., R. M. Corfield, and G. Norris (1999), Mechanisms of climate warming at the end of the Paleocene, *Science*, *285*, 724–727, doi:10.1126/science.285.5428.724.

Bijl, P. K., S. Schouten, A. Sluijs, G.-J. Reichart, J. C. Zachos, and H. Brinkhuis (2009), Early Palaeogene temperature evolution of the southwest Pacific Ocean, *Nature*, *461*(7265), 776–779, doi:10.1038/nature08399.

Bowen, G. J., D. J. Beerling, P. L. Koch, J. C. Zachos, and T. Quattlebaum (2004), A humid climate state during the Palaeocene/Eocene thermal maximum, *Nature*, *432*(7016), 495–499, doi:10.1038/nature03115.

Bowen, G. J., et al. (2006), Eocene hyperthermal event offers insight into greenhouse warming, *Eos Trans. AGU*, *87*(17), 165, 169.

Bralower, T. J. (2002), Evidence of surface water oligotrophy during the Paleocene–Eocene thermal maximum: Nannofossil assemblage data from Ocean Drilling Program Site 690, Maud Rise, Weddell Sea, *Paleoceanography*, *17*(2), 1023, doi:10.1029/2001PA000662.

Bujak, J. P., and H. Brinkhuis (1998), Global warming and dinocyst changes across the Paleocene/Eocene epoch boundary, in *Late Paleocene–Early Eocene Climatic and Biotic Events in the Marine and Terrestrial Records*, edited by M.-P. Aubry et al., pp. 277–295, Columbia Univ. Press, New York.

Carvajal-Ortiz, H., G. Mora, and C. Jaramillo (2009), A molecular evaluation of bulk organic carbon-isotope chemostratigraphy for terrestrial correlations: An example from two Paleocene–Eocene tropical sequences, *Palaeogeogr. Palaeoclimatol. Palaeoecol.*, *277*(3-4), 173–183, doi:10.1016/j.palaeo.2009.03.015.

Chanton, J. P., and F. G. Lewis (1999), Plankton and dissolved inorganic carbon isotopic composition in a river-dominated estuary: Apalachicola Bay, Florida, *Estuaries*, *22*(3), 575–583, doi:10.2307/1353045.

Clementz, M., S. Bajpai, V. Ravikant, J. G. M. Thewissen, N. Saravanan, I. B. Singh, and V. Prasad (2011), Early Eocene warming events and the timing of terrestrial faunal exchange between India and Asia, *Geology*, *39*(1), 15–18, doi:10.1130/G31585.1.

Collinson, M. E., J. J. Hooker, and D. R. Grocke (2003), Cobham lignite bed and penecontemporaneous macrofloras of southern England: A record of vegetation and fire across the Paleocene–Eocene thermal maximum, in *Causes and Consequences of Globally Warm Climates in the Early Paleogene*, edited by S. L. Wing et al., *Spec. Pap. Geol. Soc. Am.*, *369*, 333–349, doi:10.1130/0-8137-2369-8.333.

Cramer, B. S., J. D. Wright, D. V. Kent, and M.-P. Aubry (2003), Orbital climate forcing of δ^{13}C excursions in the late Paleocene–early Eocene (chrons C24n–C25n), *Paleoceanography*, *18*(4), 1097, doi:10.1029/2003PA000909.

Crouch, E. M., C. Heilmann-Clausen, H. Brinkhuis, H. E. G. Morgans, K. M. Rogers, H. Egger, and B. Schmitz (2001), Global dinoflagellate event associated with the late Paleocene thermal maximum, *Geology*, *29*(4), 315–318, doi:10.1130/0091-7613(2001)029<0315:GDEAWT>2.0.CO;2.

Crouch, E. M., G. R. Dickens, H. Brinkhuis, M.-P. Aubry, C. J. Hollis, K. M. Rogers, and H. Visscher (2003), The *Apectodinium* acme and terrestrial discharge during the Paleocene-Eocene thermal maximum: New palynological, geochemical and calcareous nannoplankton observations at Tawanui, New Zealand, *Palaeogeogr. Palaeoclimatol. Palaeoecol.*, *194*, 387–403, doi:10.1016/S0031-0182(03)00334-1.

Cui, Y., L. R. Kump, A. J. Ridgwell, A. J. Charles, C. K. Junium, A. F. Diefendorf, K. H. Freeman, N. M. Urban, and I. C. Harding (2011), Slow release of fossil carbon during the Palaeocene–Eocene thermal maximum, *Nat. Geosci.*, *4*(7), 481–485, doi:10.1038/ngeo1179.

DeConto, R. M., S. Galeotti, M. Pagani, D. Tracy, K. Schaefer, T. Zhang, D. Pollard, and D. J. Beerling (2012), Past extreme warming events linked to massive carbon release from thawing permafrost, *Nature*, *484*(7392), 87–91, doi:10.1038/nature10929.

Dickens, G. R. (2000), Methane oxidation during the late Paleocene thermal maximum, *Bull. Soc. Geol. Fr.*, *171*, 37–49.

Dickens, G. R. (2001), Carbon addition and removal during the Late Palaeocene thermal maximum: Basic theory with a preliminary treatment of the isotope record at Ocean Drilling Program Site 1051, Blake Nose, in *Western North Atlantic Paleogene and Cretaceous Paleoceanography*, edited by D. Kroon et al., *Spec. Publ. Geol. Soc. London*, *183*, 293–305.

Dickens, G. R. (2003), Rethinking the global carbon cycle with a large, dynamic and microbially mediated gas hydrate capacitor, *Earth Planet. Sci. Lett.*, *213*(3-4), 169–183, doi:10.1016/S0012-821X(03)00325-X.

Dickens, G. R. (2011), Down the rabbit hole: Toward appropriate discussion of methane release from gas hydrate systems during the Paleocene–Eocene thermal maximum and other past hyperthermal events, *Clim. Past*, *7*, 831–846, doi:10.5194/cp-7-831-2011.

Dickens, G. R., J. R. O'Neil, D. K. Rea, and R. M. Owen (1995), Dissociation of oceanic methane hydrate as a cause of the carbon isotope excursion at the end of the Paleocene, *Paleoceanography*, *10*, 965–971, doi:10.1029/95PA02087.

Dickens, G. R., M. M. Castillo, and J. C. G. Walker (1997), A blast of gas in the latest Paleocene: Simulating first-order effects of massive dissociation of oceanic methane hydrate, *Geology*, *25*(3), 259–262, doi:10.1130/0091-7613(1997)025<0259:ABOGIT>2.3.CO;2.

Diefendorf, A. F., K. E. Mueller, S. L. Wing, P. L. Koch, and K. H. Freeman (2010), Global patterns in leaf ^{13}C discrimination and implications for studies of past and future climate, *Proc. Natl. Acad. Sci. U. S. A.*, *107*(13), 5738–5743, doi:10.1073/pnas.0910513107.

Domingo, L., N. López-Martínez, M. J. Leng, and S. T. Grimes (2009), The Paleocene–Eocene thermal maximum record in the organic matter of the Claret and Tendruy continental sections (south-central Pyrenees, Lleida, Spain), *Earth Planet. Sci. Lett.*, *281*(3-4), 226–237, doi:10.1016/j.epsl.2009.02.025.

Farquhar, G. D., J. R. Ehleringer, and K. T. Hubick (1989), carbon isotope discrimination and photosynthesis, *Annu. Rev. Plant Physiol. Plant Mol. Biol.*, *40*(1), 503–537, doi:10.1146/annurev.pp.40.060189.002443.

Freeman, K. H. (2001), Isotopic biogeochemistry of marine organic carbon, in *Stable Isotope Geochemistry*, edited by J. W. Valley and D. R. Cole, *Rev. Mineral. Geochem.*, *43*, 579–605.

Freeman, K. H., and J. M. Hayes (1992), Fractionation of carbon isotopes by phytoplankton and estimates of ancient CO_2 levels, *Global Biogeochem. Cycles*, *6*, 185–198, doi:10.1029/92GB00190.

Fry, B. (2002), Conservative mixing of stable isotopes across estuarine salinity gradients: A conceptual framework for monitoring watershed influences on downstream fisheries production, *Estuaries*, *25*(2), 264–271, doi:10.1007/BF02691313.

Giusberti, L., D. Rio, C. Agnini, J. Backman, E. Fornaciari, F. Tateo, and M. Oddone (2007), Mode and tempo of the Paleocene–Eocene thermal maximum in an expanded section from the Venetian pre-Alps, *Geol. Soc. Am. Bull.*, *119*(3-4), 391–412, doi:10.1130/B25994.1.

Goericke, R., and B. Fry (1994), Variations of marine plankton δ^{13}C with latitude, temperature, and dissolved CO_2 in the world ocean, *Global Biogeochem. Cycles*, *8*(1), 85–90, doi:10.1029/93GB03272.

Gruber, N., C. D. Keeling, R. B. Bacastow, P. R. Guenther, T. J. Lueker, M. Wahlen, H. A. J. Meijer, W. G. Mook, and T. F. Stocker (1999), Spatiotemporal patterns of carbon-13 in the global surface oceans and the oceanic Suess effect, *Global Biogeochem. Cycles*, *13*(2), 307–335, doi:10.1029/1999GB900019.

Hancock, H. J. L., G. R. Dickens, E. Thomas, and K. L. Blake (2007), Reappraisal of early Paleogene CCD curves: Foraminiferal assemblages and stable carbon isotopes across the carbonate facies of Perth Abyssal Plain, *Int. J. Earth Sci.*, *96*(5), 925–946, doi:10.1007/s00531-006-0144-0.

Handley, L., P. N. Pearson, I. K. McMillan, and R. D. Pancost (2008), Large terrestrial and marine carbon and hydrogen isotope excursions in a new Paleocene/Eocene boundary section from Tanzania, *Earth Planet. Sci. Lett.*, *275*(1-2), 17–25, doi:10.1016/j.epsl.2008.07.030.

Hansen, P. J. (2002), Effect of high pH on the growth and survival of marine phytoplankton: Implications for species succession, *Aquat. Microb. Ecol.*, *28*(3), 279–288, doi:10.3354/ame028279.

Harding, I. C., et al. (2011), Sea-level and salinity fluctuations during the Paleocene–Eocene thermal maximum in Arctic Spitsbergen, *Earth Planet. Sci. Lett.*, *303*(1-2), 97–107, doi:10.1016/j.epsl.2010.12.043.

Hayes, J. M., H. Strauss, and A. J. Kaufmann (1999), The abundance of ^{13}C in marine organic matter and isotopic fractionation in the global biogeochemical cycle of carbon during the past 800 Ma, *Chem. Geol.*, *161*, 103–125, doi:10.1016/S0009-2541(99)00083-2.

Higgins, J. A., and D. P. Schrag (2006), Beyond methane: Towards a theory for the Paleocene–Eocene thermal maximum, *Earth Planet. Sci. Lett.*, *245*(3-4), 523–537, doi:10.1016/j.epsl.2006.03.009.

Hilting, A. K., L. R. Kump, and T. J. Bralower (2008), Variations in the oceanic vertical carbon isotope gradient and their implications for the Paleocene-Eocene biological pump, *Paleoceanography*, *23*, PA3222, doi:10.1029/2007PA001458.

Hollis, C. J., G. R. Dickens, B. D. Field, C. M. Jones, and C. Percy Strong (2005a), The Paleocene–Eocene transition at Mead Stream, New Zealand: A southern Pacific record of early Cenozoic global change, *Palaeogeogr. Palaeoclimatol. Palaeoecol.*, *215*(3-4), 313–343, doi:10.1016/j.palaeo.2004.09.011.

Hollis, C. J., B. D. Field, C. M. Jones, C. P. Strong, G. J. Wilson, and G. R. Dickens (2005b), Biostratigraphy and carbon isotope stratigraphy of uppermost Cretaceous–lower Cenozoic Muzzle Group in middle Clarence valley, New Zealand, *J. R. Soc. N. Z.*, *35*(3), 345–383, doi:10.1080/03014223.2005.9517789.

Hopmans, E. C., J. W. H. Weijers, E. Schefuß, L. Herfort, J. S. Sinninghe Damsté, and S. Schouten (2004), A novel proxy for terrestrial organic matter in sediments based on branched and isoprenoid tetraether lipids, *Earth Planet. Sci. Lett.*, *224*, 107–116, doi:10.1016/j.epsl.2004.05.012.

Huber, M., and R. Caballero (2011), The early Eocene equable climate problem revisited, *Clim. Past*, *7*, 603–633, doi:10.5194/cp-7-603-2011.

John, C. M., S. M. Bohaty, J. C. Zachos, A. Sluijs, S. J. Gibbs, H. Brinkhuis, and T. J. Bralower (2008), North American continental margin records of the Paleocene–Eocene thermal maximum: Implications for global carbon and hydrological cycling, *Paleoceanography*, *23*, PA2217, doi:10.1029/2007PA001465.

Kaiho, K., et al. (1996), Latest Paleocene benthic foraminiferal extinction and environmental change at Tawanui, New Zealand, *Paleoceanography*, *11*, 447–465, doi:10.1029/96PA01021.

Kelly, D. C., J. C. Zachos, T. J. Bralower, and S. A. Schellenberg (2005), Enhanced terrestrial weathering/runoff and surface ocean carbonate production during the recovery stages of the Paleocene–Eocene thermal maximum, *Paleoceanography*, *20*, PA4023, doi:10.1029/2005PA001163.

Kennett, J. P., and L. D. Stott (1991), Abrupt deep-sea warming, palaeoceanographic changes and benthic extinctions at the end of the Palaeocene, *Nature*, *353*, 225–229, doi:10.1038/353225a0.

Key, R. M., A. Kozyr, C. L. Sabine, K. Lee, R. Wanninkhof, J. L. Bullister, R. A. Feely, F. J. Millero, C. Mordy, and T. H. Peng (2004), A global ocean carbon climatology: Results from Global Data Analysis Project (GLODAP), *Global Biogeochem. Cycles*, *18*, GB4031, doi:10.1029/2004GB002247.

Knies, J., U. Mann, B. N. Popp, R. Stein, and H.-J. Brumsack (2008), Surface water productivity and paleoceanographic implications in the Cenozoic Arctic Ocean, *Paleoceanography*, *23*, PA1S16, doi:10.1029/2007PA001455.

Koch, P. L., J. C. Zachos, and P. D. Gingerich (1992), Correlation between isotope records in marine and continental carbon reservoirs near the Palaeocene/Eocene boundary, *Nature*, *358*, 319–322, doi:10.1038/358319a0.

Kopp, R. E., D. Schumann, T. D. Raub, D. S. Powars, L. V. Godfrey, N. L. Swanson-Hysell, A. C. Maloof, and H. Vali (2009), An Appalachian Amazon? Magnetofossil evidence for the development of a tropical river-like system in the mid-Atlantic United States during the Paleocene–Eocene thermal maximum, *Paleoceanography*, *24*(4), PA4211, doi:10.1029/2009PA001783.

Kump, L. R., and M. A. Arthur (1999), Interpreting carbon-isotope excursions: Carbonates and organic matter, *Chem. Geol.*, *161*(1-3), 181–198, doi:10.1016/S0009-2541(99)00086-8.

Kurtz, A., L. R. Kump, M. A. Arthur, J. C. Zachos, and A. Paytan (2003), Early Cenozoic decoupling of the global carbon and sulfur cycles, *Paleoceanography*, *18*(4), 1090, doi:10.1029/2003PA000908.

Leithold, E. L., N. E. Blair, and D. W. Perkey (2006), Geomorphologic controls on the age of particulate organic carbon from small mountainous and upland rivers, *Global Biogeochem. Cycles*, *20*, GB3022, doi:10.1029/2005GB002677.

Leon-Rodriguez, L., and G. R. Dickens (2010), Constraints on ocean acidification associated with rapid and massive carbon injections: The early Paleogene record at ocean drilling program site 1215, equatorial Pacific Ocean, *Palaeogeogr. Palaeoclimatol. Palaeoecol.*, *298*(3-4), 409–420, doi:10.1016/j.palaeo.2010.10.029.

Lourens, L. J., A. Sluijs, D. Kroon, J. C. Zachos, E. Thomas, U. Röhl, J. Bowles, and I. Raffi (2005), Astronomical pacing of late Palaeocene to early Eocene global warming events, *Nature*, *435*(7045), 1083–1087, doi:10.1038/nature03814.

Magioncalda, R., C. Dupuis, T. Smith, E. Steurbaut, and P. D. Gingerich (2004), Paleocene–Eocene carbon isotope excursion in organic carbon and pedogenic carbonate: Direct comparison in a continental stratigraphic section, *Geology*, *32*(7), 553–556, doi:10.1130/G20476.1.

Martinez, N. C., R. W. Murray, G. R. Dickens, and M. Kölling (2009), Discrimination of sources of terrigenous sediment deposited in the central Arctic Ocean through the Cenozoic, *Paleoceanography*, *24*, PA1210, doi:10.1029/2007PA001567.

März, C., B. Schnetger, and H. J. Brumsack (2010), Paleoenvironmental implications of Cenozoic sediments from the central Arctic Ocean (IODP Expedition 302) using inorganic geochemistry, *Paleoceanography*, *25*, PA3206, doi:10.1029/2009PA001860.

McCarren, H., E. Thomas, T. Hasegawa, U. Röhl, and J. C. Zachos (2009), Depth dependency of the Paleocene-Eocene carbon isotope excursion: Paired benthic and terrestrial biomarker records (Ocean Drilling Program Leg 208, Walvis Ridge), *Geochem. Geophys. Geosyst.*, *9*, Q10008, doi:10.1029/2008GC002116.

McInerney, F. A., and S. L. Wing (2011), The Paleocene–Eocene thermal maximum: A perturbation of carbon cycle, climate, and biosphere with implications for the future, *Annu. Rev. Earth Planet. Sci.*, *39*, 489–516, doi:10.1146/annurev-earth-040610-133431.

Ménot, G., E. Bard, F. Rostek, J. W. H. Weijers, E. C. Hopmans, S. Schouten, and J. S. Sinninghe Damsté (2006), Early reactivation of European rivers during the last deglaciation, *Science*, *313*(5793), 1623–1625, doi:10.1126/science.1130511.

Mook, W. G., J. C. Bommerson, and W. H. Staverman (1974), Carbon isotope fractionation between dissolved bicarbonate and gaseous carbon dioxide, *Earth Planet. Sci. Lett.*, *22*(2), 169–176, doi:10.1016/0012-821X(74)90078-8.

Murphy, B. H., K. A. Farley, and J. C. Zachos (2010), An extraterrestrial ^{3}He-based timescale for the Paleocene–Eocene thermal maximum (PETM) from Walvis Ridge, IODP Site 1266, *Geochim. Cosmochim. Acta*, *74*(17), 5098–5108, doi:10.1016/j.gca.2010.03.039.

Nicolo, M. J., G. R. Dickens, C. J. Hollis, and J. C. Zachos (2007), Multiple early Eocene hyperthermals: Their sedimentary expression on the New Zealand continental margin and in the deep sea, *Geology*, *35*(8), 699–702, doi:10.1130/G23648A.1.

Oehlert, A. M., K. A. Lamb-Wozniak, Q. B. Devlin, G. J. Mackenzie, J. J. G. Reijmer, and P. K. Swart (2011), The stable carbon isotopic composition

of organic material in platform derived sediments: Implications for reconstructing the global carbon cycle, *Sedimentology*, *59*, 319–335, doi:10.1111/j.1365-3091.2011.01273.x.

O'Regan, M., et al. (2008), Mid-Cenozoic tectonic and paleoenvironmental setting of the central Arctic Ocean, *Paleoceanography*, *23*, PA1S20, doi:10.1029/2007PA001559.

Pagani, M., K. Caldeira, D. Archer, and J. C. Zachos (2006a), An ancient carbon mystery, *Science*, *314*(5805), 1556–1557, doi:10.1126/science.1136110.

Pagani, M., N. Pedentchouk, M. Huber, A. Sluijs, S. Schouten, H. Brinkhuis, J. S. Sinninghe Damsté, and G. R. Dickens, and the Expedition 302 Scientists (2006b), Arctic hydrology during global warming at the Palaeocene–Eocene thermal maximum, *Nature*, *442*(7103), 671–675, doi:10.1038/nature05043.

Pak, D. K., and K. G. Miller (1992), Paleocene to Eocene benthic foraminiferal isotopes and assemblages: Implications for deep water circulation, *Paleoceanography*, *7*(4), 405–422, doi:10.1029/92PA01234.

Panchuk, K., A. Ridgwell, and L. R. Kump (2008), Sedimentary response to Paleocene–Eocene thermal maximum carbon release: A model-data comparison, *Geology*, *36*(4), 315–318, doi:10.1130/G24474A.1.

Pearson, P. N., B. E. van Dongen, C. J. Nicholas, R. D. Pancost, S. Schouten, J. M. Singano, and B. S. Wade (2007), Stable warm tropical climate through the Eocene epoch, *Geology*, *35*(3), 211–214, doi:10.1130/G23175A.1.

Rau, G. H., T. Takahashi, and D. J. D. Marais (1989), Latitudinal variations in plankton δ^{13}C: Implications for CO_2 and productivity in past oceans, *Nature*, *341*(6242), 516–518, doi:10.1038/341516a0.

Röhl, U., T. Westerhold, T. J. Bralower, and J. C. Zachos (2007), On the duration of the Paleocene–Eocene thermal maximum (PETM), *Geochem. Geophys. Geosyst.*, *8*, Q12002, doi:10.1029/2007GC001784.

Rost, B., K.-U. Richter, U. Riebesell, and P. J. Hansen (2006), Inorganic carbon acquisition in red tide dinoflagellates, *Plant Cell Environ.*, *29*(5), 810–822, doi:10.1111/j.1365-3040.2005.01450.x.

Schoon, P. L., A. Sluijs, J. S. Sinninghe Damsté, and S. Schouten (2011), High productivity and elevated carbon isotope fractionations in the Arctic Ocean during Eocene thermal maximum 2, *Paleoceanography*, *26*, PA3215, doi:10.1029/2010PA002028.

Schouten, S., M. Woltering, W. I. C. Rijpstra, A. Sluijs, H. Brinkhuis, and J. S. Sinninghe Damsté (2007), The Paleocene–Eocene carbon isotope excursion in higher plant organic matter: Differential fractionation of angiosperms and conifers in the Arctic, *Earth Planet. Sci. Lett.*, *258*(3-4), 581–592, doi:10.1016/j.epsl.2007.04.024.

Schouten, S., et al. (2009), An interlaboratory study of TEX_{86} and BIT analysis using high-performance liquid chromatography–mass spectrometry, *Geochem. Geophys. Geosyst.*, *10*, Q03012, doi:10.1029/2008GC002221.

Scotese, C. P., and J. Golanka (1992), Paleogeographic atlas, *PALEOMAP Progress Rep. 20-0692*, 34 pp., Univ. of Tex. at Arlington, Arlington.

Shackleton, N. J. (1986), Paleogene stable isotope events, *Palaeogeogr. Palaeoclimatol. Palaeoecol.*, *57*(1), 91–102, doi:10.1016/0031-0182(86)90008-8.

Shackleton, N. J., and M. A. Hall (1984), Carbon isotope data from Leg 74 sediments, *Initial Rep. Deep Sea Drill. Program*, *74*, 613–619, doi:10.2973/dsdp.proc.74.116.1984.

Sinninghe Damsté, J. S., W. I. C. Rijpstra, E. C. Hopmans, J. W. H. Weijers, B. U. Foesel, J. Overmann, and S. N. Dedysh (2011), 13,16-Dimethyl octacosanedioic acid (*iso*-diabolic acid), a common membrane-spanning lipid of *Acidobacteria* subdivisions 1 and 3, *Appl. Environ. Microbiol.*, *77*(12), 4147–4154, doi:10.1128/AEM.00466-11.

Sluijs, A., et al. (2006), Subtropical Arctic Ocean temperatures during the Palaeocene/Eocene thermal maximum, *Nature*, *441*(7093), 610–613, doi:10.1038/nature04668.

Sluijs, A., G. J. Bowen, H. Brinkhuis, L. J. Lourens, and E. Thomas (2007a), The Palaeocene–Eocene thermal maximum super greenhouse: Biotic and geochemical signatures, age models and mechanisms of global change, in *Deep Time Perspectives on Climate Change: Marrying the Signal From Computer Models and Biological Proxies*, edited by M. Williams et al., pp. 323–347, Geol. Soc., London.

Sluijs, A., H. Brinkhuis, S. Schouten, S. M. Bohaty, C. M. John, J. C. Zachos, G.-J. Reichart, J. S. Sinninghe Damsté, E. M. Crouch, and G. R. Dickens (2007b), Environmental precursors to light carbon input at the Paleocene/Eocene boundary, *Nature*, *450*(7173), 1218–1221, doi:10.1038/nature06400.

Sluijs, A., et al. (2008a), Eustatic variations during the Paleocene–Eocene greenhouse world, *Paleoceanography*, *23*, PA4216, doi:10.1029/2008PA001615.

Sluijs, A., U. Röhl, S. Schouten, H.-J. Brumsack, F. Sangiorgi, J. S. Sinninghe Damsté, and H. Brinkhuis (2008b), Arctic late Paleocene–early Eocene paleoenvironments with special emphasis on the Paleocene–Eocene thermal maximum (Lomonosov Ridge, Integrated Ocean Drilling Program Expedition 302), *Paleoceanography*, *23*, PA1S11, doi:10.1029/2007PA001495.

Sluijs, A., S. Schouten, T. H. Donders, P. L. Schoon, U. Röhl, G. J. Reichart, F. Sangiorgi, J.-H. Kim, J. S. Sinninghe Damsté, and H. Brinkhuis (2009), Warm and wet conditions in the Arctic region during Eocene thermal maximum 2, *Nat. Geosci.*, *2*, 777–780, doi:10.1038/ngeo668.

Sluijs, A., P. K. Bijl, S. Schouten, U. Röhl, G.-J. Reichart, and H. Brinkhuis (2011), Southern Ocean warming, sea level and hydrological change during the Paleocene–Eocene thermal maximum, *Clim. Past*, *7*, 47–61, doi:10.5194/cp-7-47-2011.

Sluijs, A., J. C. Zachos, and R. E. Zeebe (2012), Constraints on hyperthermals, *Nat. Geosci.*, *5*(4), 231, doi:10.1038/ngeo1423.

Spiker, E. C., and L. E. Schemel (1979), Distribution and stable-isotope composition of carbon in San Francisco Bay, in *San Francisco Bay: The Urbanized Estuary; Investigations into the Natural History of San Francisco Bay and Delta With Reference to the Influence of Man*, edited by T. J. Conomos, pp. 195–212, Calif. Acad. of Sci., San Francisco.

Stap, L., A. Sluijs, E. Thomas, and L. J. Lourens (2009), Patterns and magnitude of deep sea carbonate dissolution during Eocene thermal maximum 2 and H2, Walvis Ridge, southeastern Atlantic Ocean, *Paleoceanography*, *24*, PA1211, doi:10.1029/2008PA001655.

Stap, L., L. J. Lourens, E. Thomas, A. Sluijs, S. M. Bohaty, and J. C. Zachos (2010), High-resolution deep-sea carbon and oxygen isotope records of Eocene thermal maximum 2 and H2, *Geology*, *38*, 607–610, doi:10.1130/G30777.1.

Stein, R., B. Boucsein, and H. Meyer (2006), Anoxia and high primary production in the Paleogene central Arctic Ocean: First detailed records from Lomonosov Ridge, *Geophys. Res. Lett.*, *33*, L18606, doi:10.1029/2006GL026776.

Stoll, H. M. (2005), Limited range of interspecific vital effects in coccolith stable isotopic records during the Paleocene–Eocene thermal maximum, *Paleoceanography*, *20*, PA1007, doi:10.1029/2004PA001046.

Svensen, H., S. Planke, A. Malthe-Sørensen, B. Jamtveit, R. Myklebust, T. R. Eidem, and S. S. Rey (2004), Release of methane from a volcanic basin as a mechanism for initial Eocene global warming, *Nature*, *429*, 542–545, doi:10.1038/nature02566.

Thomas, D. J., J. C. Zachos, T. J. Bralower, E. Thomas, and S. Bohaty (2002), Warming the fuel for the fire: Evidence for the thermal dissociation of methane hydrate during the Paleocene–Eocene thermal maximum, *Geology*, *30*(12), 1067–1070, doi:10.1130/0091-7613(2002)030<1067:WTFFTF>2.0.CO;2.

Thomas, E., and N. J. Shackleton (1996), The Palaeocene–Eocene benthic foraminiferal extinction and stable isotope anomalies, in *Correlation of the Early Paleogene in Northwestern Europe*, edited by R. W. O. B. Knox et al., *Spec. Publ. Geol. Soc. London*, *101*, 401–441, doi:10.1144/GSL.SP.1996.101.01.20.

Uchikawa, J., and R. E. Zeebe (2010), Examining possible effects of seawater pH decline on foraminiferal stable isotopes during the Paleocene–Eocene thermal maximum, *Paleoceanography*, *25*, PA2216, doi:10.1029/2009PA001864.

Walker, J. C. G., and J. F. Kasting (1992), Effects of fuel and forest conservation on future levels of atmospheric carbon dioxide, *Palaeogeogr. Palaeoclimatol. Palaeoecol.*, *97*(3), 151–189, doi:10.1016/0031-0182(92)90207-L.

Weijers, J. W. H., S. Schouten, E. Schefuß, R. R. Schneider, and J. S. Sinninghe Damsté (2009), Disentangling marine, soil and plant organic carbon contributions to continental margin sediments: A multi-proxy approach in a 20,000 year sediment record from the Congo deep-sea fan, *Geochim. Cosmochim. Acta*, *73*(1), 119–132, doi:10.1016/j.gca.2008.10.016.

Zachos, J., M. Pagani, L. Sloan, E. Thomas, and K. Billups (2001), Trends, rhythms, and aberrations in global climate 65 Ma to present, *Science*, *292*(5517), 686–693, doi:10.1126/science.1059412.

Zachos, J. C., et al. (2005), Rapid acidification of the ocean during the Paleocene–Eocene thermal maximum, *Science*, *308*(5728), 1611–1615, doi:10.1126/science.1109004.

Zachos, J. C., G. R. Dickens, and R. E. Zeebe (2008), An early Cenozoic perspective on greenhouse warming and carbon-cycle dynamics, *Nature*, *451*, 279–283, doi:10.1038/nature06588.

Zachos, J. C., H. McCarren, B. Murphy, U. Röhl, and T. Westerhold (2010), Tempo and scale of late Paleocene and early Eocene carbon isotope cycles: Implications for the origin of hyperthermals, *Earth Planet. Sci. Lett.*, *299*(1-2), 242–249, doi:10.1016/j.epsl.2010.09.004.

Zeebe, R. E., and D. Wolf-Gladrow (2001), *CO_2 in Seawater: Equilibrium, Kinetics, Isotopes*, Elsevier, Amsterdam.

Zeebe, R. E., J. C. Zachos, and G. R. Dickens (2009), Carbon dioxide forcing alone insufficient to explain Palaeocene–Eocene thermal maximum warming, *Nat. Geosci.*, *2*, 576–580, doi:10.1038/ngeo578.